University of Stavanger

Faculty of Science and Technology

Study program/ Specialization: Petroleum Engineering - Reservoir	Spring semester, 2013
Writer: Cathrine Halvorsen	.....
Faculty supervisor: Ingebret Fjelde	
Title of thesis: The Effect of Barium and Strontium on Low Salinity Waterflooding	
Credits (ECTS): 30	
Key words: - EOR - Low Salinity Waterflooding - Ion Exchange - Ba and Sr - Mineral solubility	Pages: 84 + enclosure: 0

Acknowledgements

I will take this opportunity to thank my supervisor Ingebret Fjelde for all his help and guidance. I would also like to thank the rest of the staff at IRIS for advice and motivational words when needed.

A special thanks goes to my parents for giving me a “kick behind” when needed, and support and motivation throughout these last six years.

Abstract

Much work has been done on the subject of low salinity waterflooding (LSWF) as a potential enhanced oil recovery method. It has been shown many times that reducing the salinity of the injected brine could have a positive effect on the oil recovery. Several mechanisms have been proposed to explain why and how LSWF works, but still no mechanism has been able to explain all obtained results. However, in many cases multicomponent ion exchange has been observed to play an important role, and it has been shown to cause effects like changes in the adsorption of polar organic species and altering the wettability of a system. Both of these effects can depend on altering the ionic composition of the formation water and the injected brine.

In many laboratory experiments regarding low salinity waterflooding, potentially scale forming ions as Ba and Sr are left out of the synthetic brines to avoid in situ plugging. In this work, the effect of doing so was investigated through simulation and experimental studies, where the concentrations of Ba and Sr in the formation water were varied.

The results indicate that leaving out Ba and Sr of the FW used in experimental studies can lead to an unrepresentative initial wettability, as increasing the concentrations causes the system to become more water wet. It was also shown that the variations in Ba and Sr concentrations had an effect on potential low salinity effects.

A more systematic concentration variation, evaluating the effects of Ba and Sr alone should be performed, and also effects of Ba and SR in different COBR systems should be tested.

Table of Content:

Contents

Table of Figures:

Table of Tables:

Nomenclature:

AN – Acid number

CEC – Cation exchange capacity

COBR – Crude oil, Brine, Rock

dP – Pressure drop across the core

DV – Dead volume of the flooding rig

EDL – Electric double layer

EOR – Enhanced Oil Recovery

FW – Formation water

ICP – Inductive coupled plasma

IFT – Interfacial tension

k_{ro} – Oil relative permeability

$k_{ro}(S_{wi})$ – Oil relative permeability at initial water saturation

k_{rw} – Water relative permeability

$k_{rw}(S_{or})$ – Water relative permeability at residual oil saturation

LS – Low salinity

LSW – Low salinity water

LSWF – Low salinity waterflooding

MIE – Multicomponent ion exchange

NPD – Norwegian Petroleum Directorate

N_c – Capillary number

OOIP – Original oil in place

P_c – Capillary pressure

PV – Pore volume

STO – Stock tank oil

S_o – Oil saturation

S_{or} – Residual oil saturation

S_{we} – Water saturation at the end of flooding

S_{wi} – Initial water saturation

1. Introduction

Water injection has been used to increase oil recovery since the late 1800's. Initially it was thought that the increased recovery was a strictly mechanical effect, caused by pressure maintenance and displacement. However, work done by Tang and Morrow (1996, 1997, 1999) indicated that lowering the salinity of the injected brine could increase the oil recovery. In the later years, much research has been done on low salinity (LS) water injection both in the lab and in field tests. (Morrow et al. 1998, Tang and Morrow 1999, McGuire et al. 2005, Lager et al. 2006, Seccombe et al. 2008). This has resulted in the conclusion that injecting LS brine could indeed lead to more oil being recovered. Many attempts have been made to explain why and how low salinity water flooding (LSWF) works (more details in section 2.7), but still there is no single mechanism that has been able to explain all experimental results.

In the later years, experiments have been performed indicating that not only the salinity of the injected brine will have an effect, but also the chemical composition (Suijkerbuik et al. 2012, Fjelde et al. 2013a). Suijkerbuik et al. (2012) showed that varying the concentrations of different ions would lead to different wettability alterations, even though the salinity was kept constant. The work done by Fjelde et al. (2013a) indicated that the LS effect could depend on the amount of divalent ions present on the clay surface. And as different clays show different affinity for different ions (Dolcater et al. 1968), this may also indicate that the types of ions present in the injected brine could play a role.

In most LSWF laboratory experiments, potentially scale forming divalent cations, such Ba and Sr, are left out of the artificial formation water (FW) to avoid in-situ plugging. If the results showed by Suijkerbuik et al. (2012) and Fjelde et al. (2013a) are correct, this may give a misleading image the amount of divalent ions on the clay surface and hence give an unrepresentative image of the wettability after aging.

The objective of this thesis is to explore whether the presence of Ba and Sr in the formation water will have any effect on initial wettability of a core and/or wettability alteration and recovery during a LSWF. Rock, oil and brines similar to Fjelde et al. (2012 and 2013a) are used. Concentrations of Ba and Sr in the FW are chosen by simulation. The formation brines are composed to avoid precipitation, and the injected low salinity brine is the one showing the lowest concentration of divalent ions on the clay surface after flooding.

2. Theory

2.1– Classical Steps in Oil Recovery

Traditionally, oil recovery has been divided into the stages; primary, secondary and tertiary (Green and Willhite, 1998). They described the production in a chronological sense.

2.1.1 – Primary Recovery

The first recovery stage relies on the natural displacement energy of the reservoir to drive the oil towards the well (Green and Willhite, 1998). These natural energy sources are (Green and Willhite 1998, Glover 1997):

- solution-gas drive
- gas-cap drive
- natural water drive
- fluid and rock expansion
- gravity drainage
- combination or mixed drive

The recovery efficiency from this stage is usually low, and the pressure in the formation may decrease rapidly resulting in solution gas formation (Zolotukhin and Ursin, 2000).

2.1.2 – Secondary Recovery

When the natural drive has diminished to unreasonably low efficiencies, it is augmented by injecting water or immiscible gas to displace oil towards the producing wells (Green and Willhite 1998, Glover 1997). Water injection is much more efficient than immiscible gas injection, and today, secondary recovery is almost synonymous with water injection.

2.1.3 – Tertiary Recovery

Primary and secondary recovery methods usually don’t recover more than 35% of the original oil in place (OOIP) (Glover 1997, Green and Willhite 1998). The tertiary stage includes all the oil that is recovered, after secondary injection is no longer economically feasible. Tertiary processes include miscible gasses, chemicals and/or thermal energy to displace more oil when the secondary water injection has become uneconomical.

Today however, many reservoir production operations are not conducted in this specific order. A so-called tertiary process may for example be implemented instead of regular water injection. This has led to the use of the term "enhanced oil recovery" (EOR).

2.2– EOR

The Norwegian Petroleum Directorate (NPD) defines EOR as a term used for advanced methods of reducing the residual oil saturation in the reservoir (NPD 2013). The processes involve the injection of a fluid or fluids into the reservoir to supplement the natural energy as well as to interact with the crude oil/rock/brine (COBR) system to obtain favorable conditions for additional oil recovery (Green and Willhite, 1998). These interactions might, for example, lead to reduced interfacial tensions (IFT), oil swelling, reduction of oil viscocity, wettability alteration or favorable phase behavior.

The main objectives for EOR are (Zolotuchin and Ursin 2000, Green and Willhite 1998)

- Maintain reservoir pressure at a desired level
- Enhance displacement efficiency by reducing the residual oil saturation – improving the effectiveness of the displacing fluid to mobilize the oil in the places in the formation where it reaches the oil (microscopic sweep efficiency).
- Improve sweep efficiency by improving the mobility ratios between all displacing and displaced throughout the process – improve the injected fluids ability to contact the reservoir in a volumetric sense (macroscopic sweep efficiency).

An ideal EOR process would contact the entire reservoir removing all oil from the pores contacted by the fluid – residual oil saturation (S_{or}) will be zero.

2.3– Displacement Forces

In LSWF, oil is displaced by an immiscible fluid. The main forces acting on the fluids, having an impact on displacement efficiency are; gravity forces, viscous forces and capillary/interfacial forces (Bavière 1991, Green and Willhite 1998, Glover 1997). The interplay among the forces will to a large extent govern the residual saturations in a porous medium.

2.3.1 – Gravity Forces

The density differences between the fluid phases, will lead to the arise of gravity forces (Green and Willhite 1998). It can be described by equation 2.1:

$$\nabla P_g = \Delta\rho g \sin\alpha \qquad 2.1$$

Where ∇P_g is the pressure gradient due to gravity, $\Delta\rho$ is the density difference between the phases, g is the gravitational acceleration and α is the dip angle of the formation. The gravity forces will be more severe for cases where there is a large density difference between the phases, and where there is a large dip in the formation.

2.3.2 – Viscous Forces

The viscous forces in a porous medium are reflected in the magnitude of the pressure drop that occurs as a result of flow of a fluid through the medium (Green and Willhite 1998). Viscous force in a porous medium can be expressed in terms of Darcy's law (equation 2.2);

$$\Delta p = -\frac{\bar{v}\mu L\varphi}{k} \qquad 2.2$$

Where Δp is the pressure drop across the porous medium, $\bar{v}$ is the average velocity of fluid in the pores, μ is the fluid viscosity, L is the length of the porous medium and k is the permeability of the porous medium.

2.3.3 – Capillary Forces

Whenever immiscible phases coexist in a porous medium, surface energy related to the fluid interfaces influences the saturations, distributions and displacement of the phases (Green and Willhite 1998). Capillary forces are exerted by the fluid-fluid interface where the droplet is bounded by another fluid (Bavière 1991). This force, which is a tensile force, is quantified in the terms of IFT. IFT is defined as the force per unit length required to create additional interfacial area (Green and Willhite 1998).

Capillary forces and IFT depend on the physical properties of the interface, as well as the surface deformation (Bavière 1991). At pore scale, capillary forces are much larger than the other forces, and are therefore often the controlling factor of fluid distribution.

2.3.4 – Capillary Number

The outcome of a flooding process is determined by the interplay from all of the forces, and the relative magnitudes of them are very important for the recovery obtained in a core flood (Green and Willhite 1998). One way of expressing this is through the capillary number (N_c), which is the ratio of the viscous to the capillary forces. This can be expressed as shown in equation 2.3:

$$N_c = \frac{F_v}{F_c} = \frac{v\mu_w}{\sigma_{ow}\cos\theta} \qquad 2.3$$

It has been shown that increasing N_c can lead to a reduction in residual oil saturation (Green and Willhite 1998). This can be achieved by: increasing viscosity of displacing fluid, reducing the IFT, increasing the flooding velocity (usually not an option in reservoir scale), or by altering the wettability.

2.4– Wettability

Fluid distribution in a porous medium is not only affected by the forces at fluid/fluid interfaces, but also by the forces at fluid/solid interfaces (Green and Willhite 1998). When two immiscible fluids are in contact with a solid surface, there is a tendency for one of the fluids to be preferred by the surface. The preferred phase is termed the wetting phase, the other is termed the non-wetting phase.

A COBR system can either be water-wet, oil-wet or intermediate/mixed-wet (Green and Willhite, 1998). In a water-wet core, containing low viscosity oil, there is typically water filling the small pores and a water film lining the walls of the large pores, leaving the oil phase to reside in the middle as shown in *Figure 1* (Green and Willhite 1998). When flooded by water, the water phase maintains a fairly uniform front, displacing the oil in front of it (Anderson 1986). The connection of the oil will become weaker and eventually break off, leaving some residual oil trapped in the center of the pores surrounded by water. In a system containing oil with low viscosity, almost all of the remaining oil is immobile, and hardly any more oil is produced after water breakthrough (Agbalaka and Dandekar 2008).

In an oil-wet system, oil is typically occupying the small pores as well as wetting the walls of the larger pores, while the water occupy the center of the larger pores, as shown in *Figure 1*. During waterflooding, channels or fingers of water will form through the center of the larger

pores, pushing the oil in front of them (Anderson 1986). The water breaks through early, and most of oil will be recovered after water breakthrough.

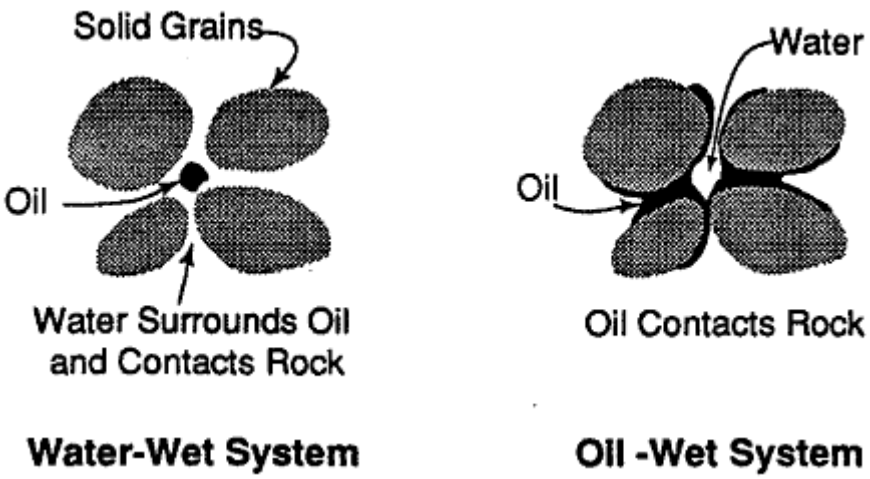

Figure 1 - Effect of wettability on fluid distribution in water wet and oil wet system (Green and Willhite, 1998)

Intermediate wettability occurs when both fluids shows tendencies of wetting the formation, one only slightly more than the other (Green and Willhite 1998). Mixed wettability results from variation or heterogeneity in chemical composition of the rock leaving some parts of the core water-wet, and some parts oil-wet. This result in a reduced recovery at breakthrough compared to water-wet cores, but with extended production after breakthrough (Donaldson and Alam 2008).

In theory, a simple way of determining the wettability state is by measuring the contact angle between the fluids interface and the solid surface through the water phase as shown in *Figure 2* (Green and Willhite 1998, Glover 1997). In terms of contact angle, Zolotukin and Ursin (2000) classified the wettability states as given in *Table 1*. This is however difficult in reservoir rock due to the complexity of the pore structure. In the petroleum industry, it is more usual to describe changes in the capillary pressure and relative permeability curves as shown in *Figure 5*. This will be further looked into in the following sections.

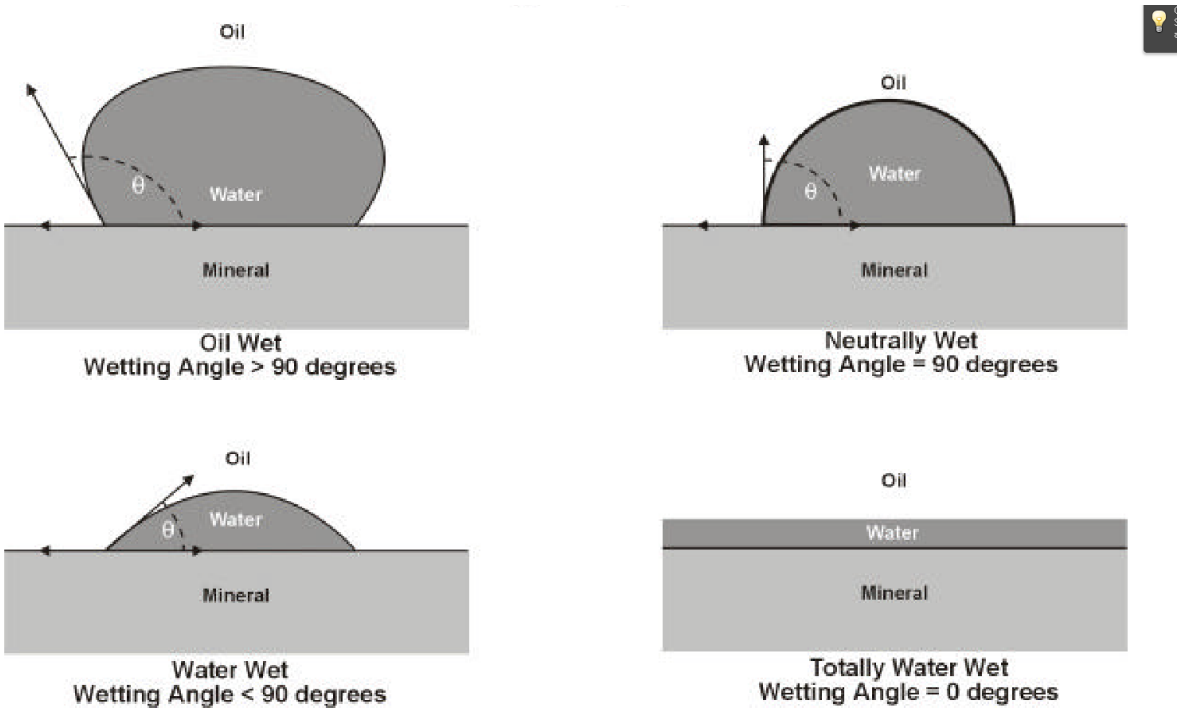

Figure 2 - Contact angles for various wetting properties (Glover, 1997)

Contact angle values [degrees]:	**Wettability state:**
0-30	Strongly water-wet
30-90	Preferentially water-wet
90	Neutral wettability
90-150	Preferentially oil-wet
150-180	Strongly oil-wet

Table 1 - Wettability expressed by contact angles (Zolotukin and Ursin, 2000)

There are many factors affecting the wettability of a COBR system (Green and Willhite 1998, Bavière 1991, Zolotukin and Ursin 2000):

- Rock mineral composition
- Pore structure
- Pore geometry
- Pore size
- Brine composition
- Salinity
- pH
- Temperature
- Oil composition

They all affect wettability in different ways, and to isolate the parameters in wettability studies are difficult. Suijkerbuijk et al. (2012) concluded that wettability is a property of a COBR ensemble, rather than a function of a single variable. Conclusions made for a particular ensemble may not necessarily apply for other COBR systems.

The wettability is an important factor when evaluating the fluid entrapment, flow and distribution in a pore space (Bavière 1991). This is due to its influence on capillary pressure, fluid saturations and relative permeability characteristics. Relative permeability curves and capillary pressure curves may be used to characterize the wettability of a system (Anderson 1986).

Wettability alteration in one of the dominant mechanisms of many EOR methods (Nasralla et al. 2011). It is widely accepted that mixed-wet conditions usually result in the lowest S_{or} values after injection of several pore volumes (Green and Willhite 1998). For field applications S_{or} may not be reached as it is it not feasible to inject several pore volumes (PV) of fluid into the reservoir.

2.5– Relative Permeability

Usually, permeability measurements are made with a single fluid filling the pores (Glover, 1997). In petroleum reservoirs, this is rarely the case, as two, and sometimes three, phases tend to be present. If more than one phase is present, one would expect the permeability to either fluid to be lower than for the single fluid, since part of the pore space is occupied by the other fluid(s). The relative permeability of a particular fluid is the ratio of its effective permeability at a particular saturation to the absolute permeability of the system, as given by equation 2.4 (Glover, 1997). Here, k_{rf} represents relative permeability of the investigated fluid. The sum of the relative permeabilities in a system is always ≤ 1.

$$k_{rf} = \frac{kef}{k} = \frac{effective\ fluid\ permeability}{absolute\ permeability} \qquad 2.4$$

In laboratory tests, one fluid is displaced by another, and hence the effective permeabilities are measured over a range of saturations enabling construction of relative permeability. curves. Typical relative permeability curves for a water-wet and an oil-wet system are shown in *Figure 3*.

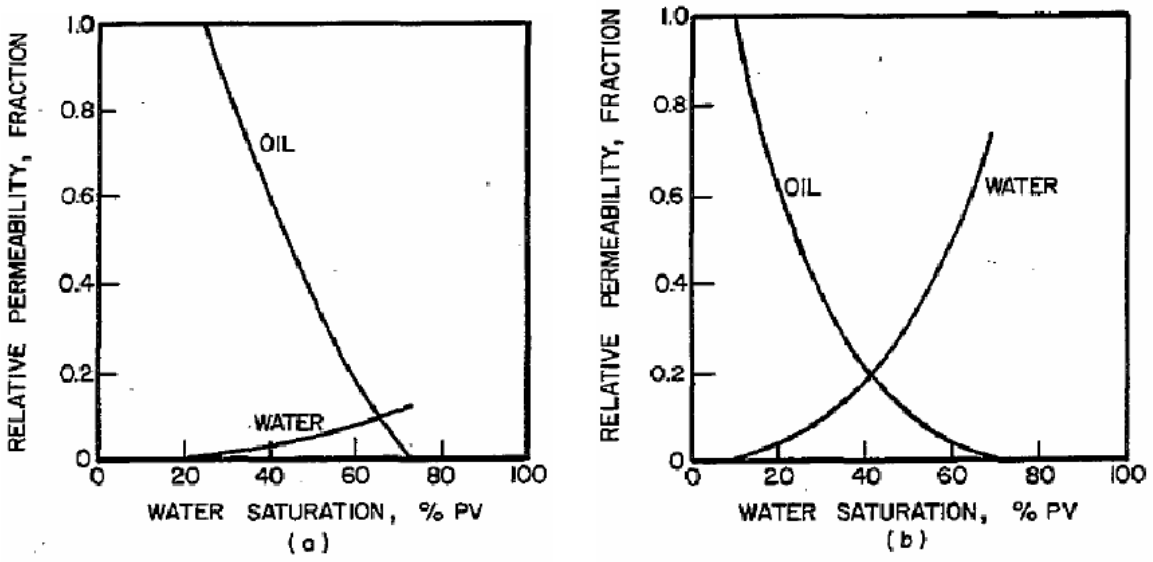

Figure 3 - Relative permeability curve for a (a) water-wet and (b) an oil-wet system (Anderson 1986)

The relative permeabilities of a COBR system depend strongly on the wettability (Green and Willhite 1998). Most systems fall somewhere between the two extremes of totally water-wet, and totally oil-wet (Glover 1997). However, knowledge of the two extreme cases will make interpreting intermediate data easier.

Here, three stages of flooding water-wet and oil-wet cores, containing low viscous oil, will be compared; start (at initial water saturation (S_{wi})), during and end (at S_{or}) (Glover 1997). An example of relative permeability curves for a water-wet vs. a mixed-wet system is shown in *Figure 5*.

Start:

In a water-wet system the water will not flow at S_{wi}; oil relative permeability $(k_{ro}) = 1$ and water relative permeability $(k_{rw}) = 0$.

In an oil-wet system an applied pressure differential is required for the water to enter the pores.

During:

In a water-wet system, the injected water migrate in a piston-like manner, causing extended production after breakthrough to be limited.

In an oil-wet system the injected water flows through the largest flow channels first causing an earlier breakthrough than for the water-wet system. k_{ro} falls and k_{rw} rises rapidly, but production is maintained long after initial water breakthrough.

End:

In a water-wet system, most of the oil is produced prior to the water breakthrough, and hence S_{or} is reached soon after breakthrough.

In an oil-wet system, a very large volume of water is needed before S_{or} is reached.

Intermediate/mixed wet systems will give rel-perm curves somewhere in between the two extreme cases. A change in wettability will alter the curves one way or the other depending on the change being towards more water-wet or more oil-wet.

2.6– Capillary Pressure

Because the interface between two immiscible fluids is in tension, a pressure difference exists across the interface (Green and Willhite 1998). This pressure difference is known as the capillary pressure (P_c). P_c can be calculated from equation 2.5:

$$P_c = \frac{2\sigma_{ow}\cos\theta}{r} \qquad 2.5$$

σ_{ow} is the IFT between oil and water, θ is the contact angle between water and the solid, and r is the radius of the capillary/pore. Hence, the defined capillary pressure is a function of IFT, the wetting condition (through θ) and pore size.

Plateau also developed the more complex expression for calculating P_c shown in equation 2.6 (Green and Willhite, 1998):

$$P_c = \sigma\left(\frac{1}{r_1} + \frac{1}{r_2}\right) \qquad 2.6$$

Where r_1 and r_2 are the radii of curvature as shown in *Figure 4*:

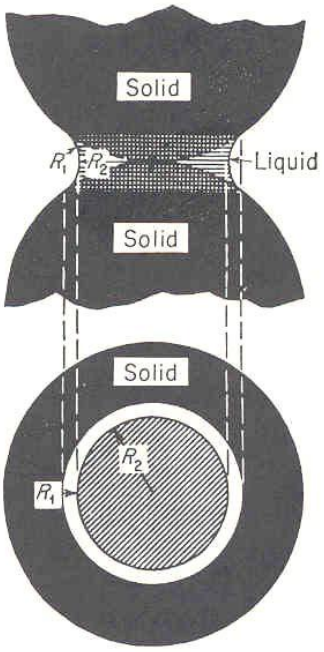

Figure 4 - Wetting of spheres showing radii of curvature to use in equation 2.6 (Green and Willhite, 1998)

In a porous medium, there are many factors affecting the capillary pressure (Castellan, 1983). Some examples of such factors are:

- Pore size and geometry
- Interfacial tension of the two immiscible fluids
- The wetting condition
- Saturation and saturation history

Capillary pressure can both aid and disrupt fluid displacement in a porous medium and it also determines the saturation distribution (Castellan 1983). At the end of a flooding process, P_c is usually 0 at the outflow end. The water saturation at this point is therefore determined by $P_c(S_{we}) = 0$. If S_{we} (water saturation at the end of the flooding) is sufficiently low, this may give a wrong image of the average water saturation in the rest of the core at the end of the flooding. This is often the case if the core is short and/or the flooding rate is low. This effect is called the "capillary end effect".

2.6.1 – Capillary Pressure Curves

Due to the complexity of pore structure in a formation, it is impossible to use equations 2.4 and 2.5 to calculate the capillary pressure in a porous media (Engler 2012). P_c is therefore measured as a function of the saturation of the wetting phase, and capillary pressure can be viewed as the necessary pressure to force non-wetting fluid to displace the wetting fluid. In a P_c curve plot, as shown in the upper part of *Figure 5*, it is usual to present two curves: the imbibition curve and the drainage curve. The imbibition curve represents displacing of the non-wetting phase by the wetting phase, and the drainage curve represents non-wetting phase displacing wetting phase. As the wetting fluid has a natural tendency to saturate the rock, the imbibition curve will present a lower P_c than the drainage curve for a given saturation. Also, $P_c > 0$ is required to force the non-wetting fluid into the rock. (Engler 2012, Abdallah et al. 2007)

The capillary pressure curve will be altered if the wettability conditions change. For example, the imbibition and drainage curves for a strongly water-wet system are positive over most of the saturation range, indicating spontaneous imbibition of water, while in a mixed wet system the curves have both positive and negative portions, indicating that spontaneous imbibition of

both phases can occur (Abdallah et al. 2007). Many EOR methods cause a wettability alteration which can be characterized using the capillary pressure curve.

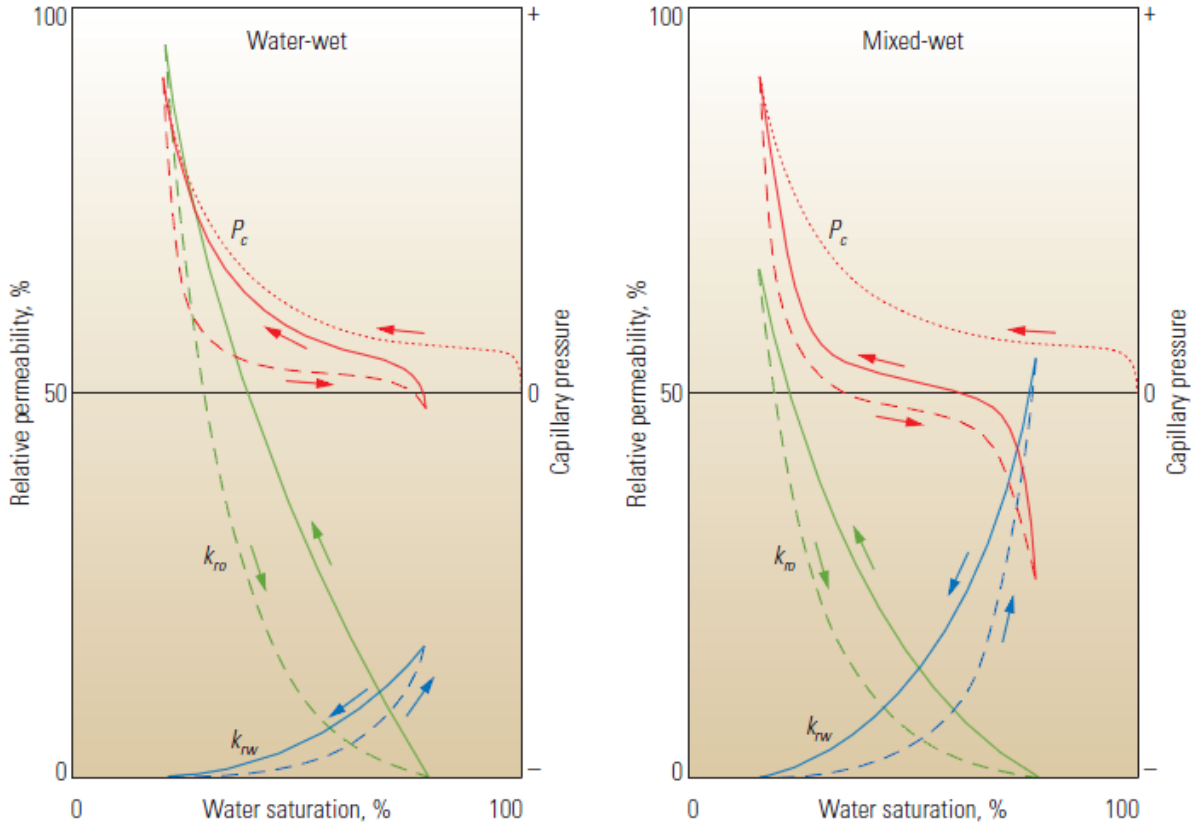

Figure 5 - Capillary Pressure and Relative Permeabilty Curves for Water-Wet (left) and Mixed-Wet (right) systems. (the dotted curves represent primary drainage, the dashed curves represent imbibition and the continous curves represent drainage (Abdallah et al. 2007)

2.7– Low Salinity Water Flooding

Low salinity water injection is an EOR method consisting of injecting water of lower salinity than the formation brine into a reservoir. It originates from work done by Bernard (1967) showing improved oil recovery after flooding with fresh water. Later Jadhunandan and Morrow et al. (1990, 1991) and Morrow (1996) showed that composition of the injected brine could have an effect on oil recovery. Tang and Morrow (1997 and 1999) worked further on this idea, and they performed experiments indicating that injecting brine with low salinity could be beneficial.

Since then, much work has been done on the subject. Results from both laboratory work and field tests, have shown that reducing salinity of the injected water can increase the oil recovery (Morrow et al. 1998, Tang and Morrow 1999, McGuire et al. 2005, Lager et al. 2006, Seccombe et al. 2008). It has also been shown that LSWF can be effective both as a secondary and a tertiary flood.

A set of criteria for LSWF to work has been listed in the literature (Morrow and Buckley, 2011):

- Presence of formation water containing multivalent cations
- Polar components in the oil
- Active clay on/in the rock

However, even though all of these criteria are fulfilled, there have been examples of cases where injection of low salinity water (LSW) showed little or no effect (Skrettingland et al. 2011, Morrow and Buckley 2011). Hence the criteria are considered to be necessary, but not sufficient.

A list of causing mechanisms has been proposed during the years:

- Migration of mixed wet clay particles (Tang and Morrow, 1998)
- pH increase and alkaline like flooding (McGuire et al. 2005)
- Expansion of the electrical double layer (Ligthelm et al. 2009)
- Local pH increase (Austad et al. 2010)
- Multicomponent ion exchange (MIE) (Lager et al. 2006)

But so far, no mechanism has been recognized as the “true” one, as none of them can explain all the obtained experimental results. The reason for the “confusion” is probably the

complexity of the COBR interactions in the reservoir, and hence the many parameters involved. Both Morrow and Buckley (2011) and Austad et al. (2010) have made the suggestion that the low salinity effect probably is a result of different mechanisms acting together.

2.7.1 – Proposed Mechanisms

Release of fines/Mixed Wet Clay Particles

The first mechanism proposed was put forward by Tang and Morrow (1999). It suggested that the increased oil recovery was caused by the release of oil bearing fines. The clay particles remain undisturbed as long as they are contacted by high salinity brine, leaving them with their oil-wet nature (Lager et al. 2006). As low salinity water in injected, clay particles detach from the pore surface, exposing underlying surfaces, increasing the water-wetness of the system. Tang and Morrow (1999) supposed that releasing of these mixed wet clay particles, as shown in *Figure 6*, mobilized previously retained oil droplets, increasing the oil recovery.

The migration of fines is also related to a permeability reduction due to plugging of pores (Tang and Morrow 1999). This plugging may make the water "change its path", causing unswept areas to be reached by water, and hence increasing oil recovery even more.

However, many LSWF experiments, with positive results, having neither traces of fines in the effluent or reduction in permeability (Lager et al. 2006, Morrow and Buckley 2011). This has caused the migration of fines to be considered as a side effect, rather than a causing mechanism.

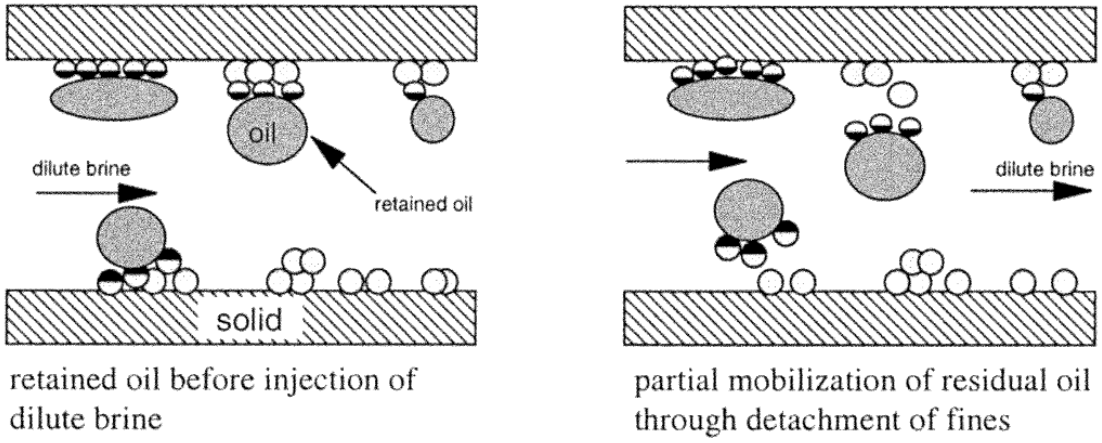

Figure 6 - Mobilization of mixed-wet clay particles during LSWF (Tang and Morrow, 1999)

pH Increase

Many low salinity studies show a significant pH increase. Based on this, McGuire et al. (2005) proposed a mechanism indicating that a sufficient rise in pH could make the LSWF act like an alkaline flooding.

The rise in pH is caused by two concomitant reactions: carbonate dissolution and cation exchange between the clay minerals and the invading water (Lager et al. 2006). The dissolution of carbonates will result in an excess of OH^- increasing the pH, caused by the following reactions:

$$CaCO_3 \leftrightarrow Ca^{2+} + {CO_3}^{2-}$$

$${CO_3}^{2-} + H_2O \leftrightarrow {HCO_3}^- + OH^-$$

The dissolution reactions are slow, and are depending on the carbonate mineral concentration present in the rock. The cation exchange reaction is much faster. H^+ ions present in the water will exchange with cations previously adsorbed to the clay, causing the pH to rise.

If the pH is elevated to 9 or more, this would make the LSWF act like an alkaline flooding where surfactants are generated in-situ (McGuire et al. 2005). This causes an alteration of the wettability and IFT which control the forces holding the oil in the pores. The surfactants can also alter the wettability of the system, and it may also act as an emulsifying agent bringing dispersion of oil into the water.

However, it is widely accepted that for an alkaline process to work, the acid number (AN) of the oil must be above 0.2 (Lager et al. 2008). Some of the best results from LSWF are from reservoirs containing oil with very low acid numbers (AN<0.05). Also, according to Lager et al. (2008), no experiments showing a pH increase has been performed at reservoir conditions with live fluids. Most reservoirs contain CO_2, which will act like as a pH buffer, and reaching a pH of 9 or more is unlikely.

Double Layer Expansion

Expansion of the electrical double layer (EDL) was proposed as a possible explaining mechanism by Ligthelm et al. (2009).

The structure of ions in a solvent adjacent to a charged solid is described by the EDL (Lee et al. 2010). In the layer closest to the surface charge the ions are strongly bound, while in the second layer, the ions are in motion in the adjacent liquid, but the concentration of ions is higher than in the rest of the fluid, as illustrated in *Figure 7*.

The thickness of the EDL is defined as the distance over which the concentration of the ions differs from the bulk value (Lee et al. 2010). This thickness is dependent of electrolyte concentration and ion valency – low ionic strength and ion valencies lead to a thicker double layer.

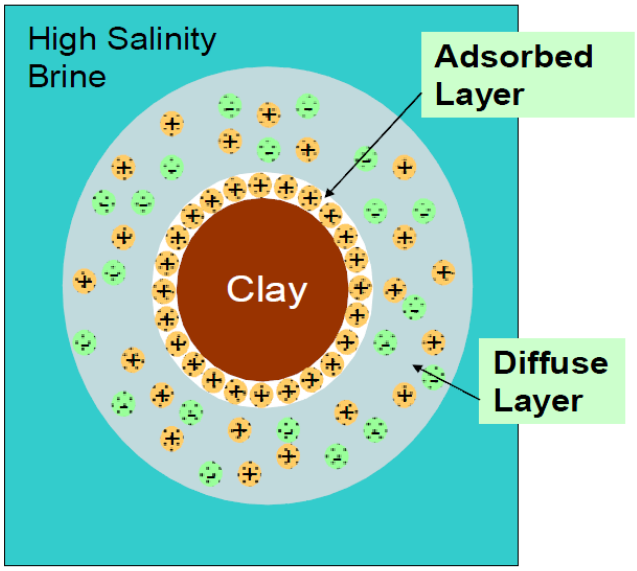

Figure 7 - The electrical double layer (Lee et al. 2010)

Polar organic components can bond to the negative clay surface either directly (positive components) or by cation bridging (negative components) (Lee et al. 2010). The high salinity brine might retain the oil components, but as the LSW is injected, the divalent cations on the clay surfaces will be exchanged by monovalent cations. The decrease in ionic strength on the clay surface will cause the EDL thickness to increase, thickening the water film surrounding the clay (as shown in *Figure 8*) and making it more water-wet.

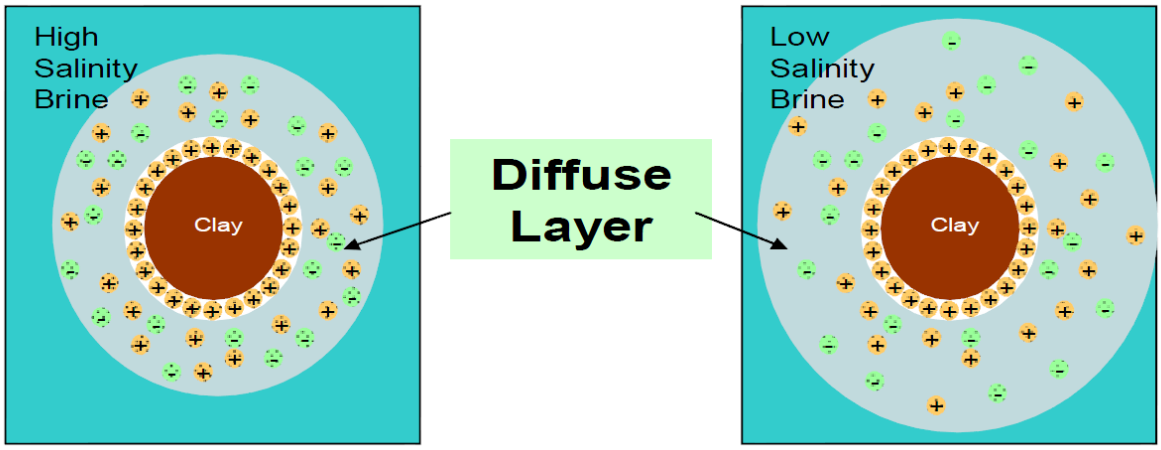

Figure 8 - Effect of salinity on EDL (Lee et al. 2010)

Local pH Increase

In 2010, Austad et al. put forward a chemical mechanism explaining the low salinity effect by a local pH increase. They assumed that the EOR effect of LSWF is caused by improved water wetness, and that parameters as clay properties, polar components in the crude oil and the initial formation water (FW) composition and pH will play a major role in the process.

The clay acts as a cation exchanger, where initially both acidic and basic organic material are adsorbed together with inorganic cations from the FW. At reservoir conditions, an equilibrium is established. When low salinity brine is injected, this equilibrium is disturbed and a net desorption of cations occur. To compensate for this loss of cations, H^+ ions from the water, close to the clay surface, are adsorbed. This induces a local pH increase close to the clay surface, causing the reactions between adsorbed acidic and basic material as shown in equations 2.7 and 2.8:

$$Clay - NHR_3^+ + OH^- = Clay + R_3N + H_2O \qquad 2.7$$

$$Clay - RCOOH + OH^- = Clay + ROOC^- + H_2O \qquad 2.8$$

The proposed mechanism for desorbing the acidic and basic components is illustrated in *Figure 9*.

Suijkerbuijk et al. (2012) however, rejected this mechanism as a full explanation to the low salinity effect. They performed experiments injecting brine with lower pH than the formation brine, still showing an increase in oil recovery. They also showed results indicating that increasing the Mg concentration in the formation brine will make the rock more oil-wet. Hence, the Mg will aid the oil in binding to the surface. In Austad's mechanism on the other hand, the oil and the Mg will compete for the adsorption sites.

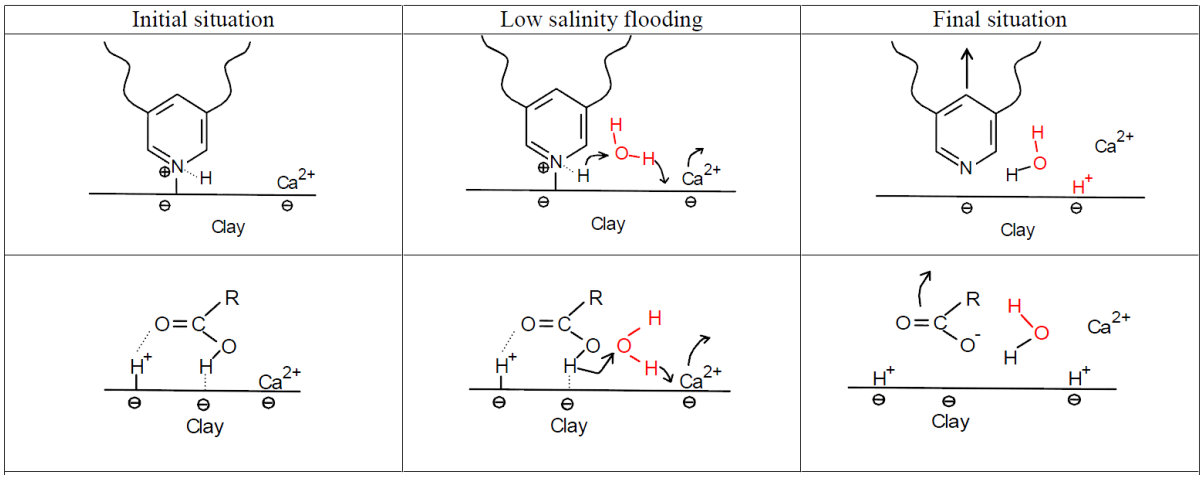

Figure 9 – Local pH increase mechanism. Upper: Desorption of basic material. Lower: Desorption of acidic material. The initial pH at reservoir conditions may be in the range of 5. (Austad et al. 2010)

Multicomponent Ion Exchange

The MIE mechanism was put forward by Lager et al. in 2006. They performed geochemical analysis on the low salinity effluents, indicating that MIE chromatography play a dominant role for the water chemistry during flooding. The basis of chromatography is that all ions in the pore water compete for the mineral exchange sites (Lager et al. 2008). And as the natural exchangers show different affinity for the different cations, the ratio of sorbed over solute concentration will vary for each cation type.

There are eight possible mechanisms that may cause adsorption of organic matter onto clay (Lager et al. 2006):

- Cation exchange
- Protonation
- Anion exchange
- Water bridging
- Cation bridging
- Ligand exchange
- Hydrogen bonding
- Van der Waals interactions

It has been shown that, out of these, ligand exchange, Van der Waals interactions and cation bridging dominates in regard to adsorbing organic matter onto clay surfaces, as shown in *Figure 10*.

On an oil-wet surface, some organic components will be adsorbed to the clay surface through bonding between polar components in the oil and already adsorbed multivalent cations. At the same time, some organically polar compounds will be adsorbed directly on the clay surface. The injection of LSW, will through MIE, replace both the binding divalent cations and the polar components, and replace them with uncomplexed cations. This will lead to a more water-wet surface, increasing oil recovery.

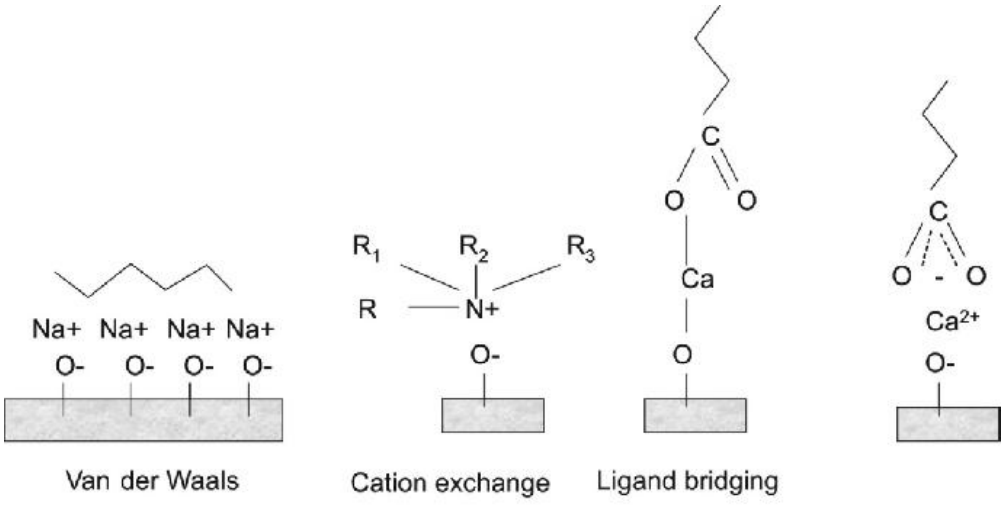

Figure 10 – The diverse adhesion mechanisms occurring between clay surface and crude oil (Lager et al. 2008)

2.8– Clays and Affinity to Ions

The presence of clay was listed by Tang and Morrow (1999) as one of the criteria for LSWF to increase oil recovery. Clay minerals are generally crystalline in nature, and their properties are determined by the structure of the clay crystals. Clay minerals can generally be divided into four different main groups (da Costa Ferriera 2012, Austad et al. 2010); Kaolinite, Illite, Montmorillonite and Chlorite. Properties of the different clay types are listed in *Table 2*:

Property:	**Kaolinite:**	**Illite/Mica:**	**Montmorillonite:**	**Chlorite:**
Layers (Si:Al):	1:1	2:1	2:1	2:1:1
Particle size [micron]:	5-0.5	Large sheets to 0.5	2-0.1	5-0.1
CEC [meq/100g]:	3-15	10-40	80-150	10-40
Surface area BET-N_2 [m^2/g]:	15-25	50-110	30-80	140

Table 2 - Properties of actual clay minerals (IDF 1982)

Common sandstone reservoir clays commonly have a crystal structure made up of sheets of tetrahedral silica and octahedral aluminum layers (Austad et al. 2010). See *Figure 11* Structural charge imbalances, either in the silica or in the aluminum layer and also on the end surfaces, cause a negative charge on the clay surface. This makes the clay a natural cation exchanger.

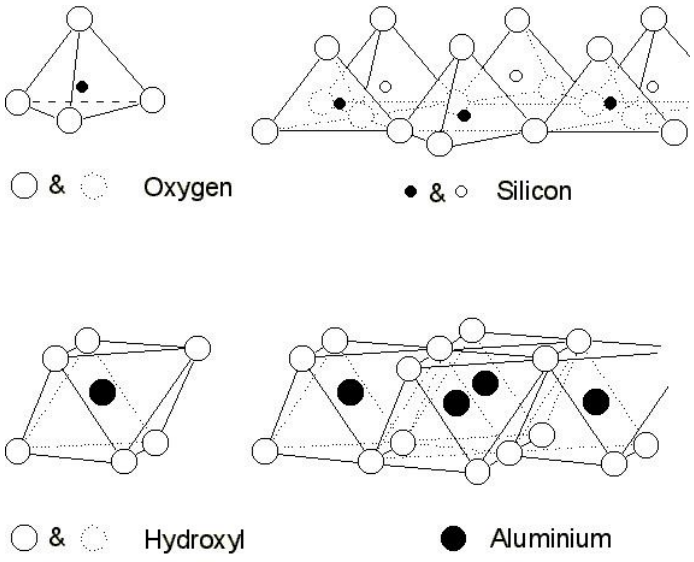

Figure 11 – Common sandstone reservoir clays crystal structure. Upper: Tetrahedral silica, Lower: Octahedral aluminum (www.groundwaterresearch.com.au)

Cation exchange capacity (CEC) is defined as the degree of which a clay can hold and exchange cations (Tree Fruit Soil and Nutrition 2004). Different clay types have different CEC, and they also show different affinities towards different ions (Dolcater et al. 1968). Generally, the relative affinity for cations is believed to be Li < Na < K < Mg < Ca < Sr < Ba < H (IDS 1982, Suarez and Zahow 1989, Bennet 2013). This means that at equal concentrations, Ca will be more successful at replacing K, than K will be at replacing Ca. However, it is possible for a cation with lower affinity to replace a cation of higher affinity if the concentration of the low affinity cation is sufficiently high. Guoy theory predicts that the double layer contains a much higher concentration of multivalent ions relative to monovalent ions, due to charge density (Bennet 2013). However, this preference for divalent ions decreases with increasing ionic strength. I.e. In seawater, the dominant exchangeable cation is Na, while in dilute waters, the dominant exchangeable cation is Ca.

2.9– Possible Effects of Ba and Sr Present

There have been several studies showing that salinity of the injected brine is not the only important factor in LSWF (Nasralla et al. 2011, Suijkerbuijk et al. 2012, Fjelde et al. 2013a). The chemical composition of the injected water, as well as the initial formation water, may play a role in whether the low salinity effect will be obtained or not. Suijkerbuijk et al. (2012) performed experiments where the relative concentration of Ca and Mg was varied. The results showed that using a Ca rich formation brine during aging would lead to a less water-wet system than a Mg rich formation brine. This led them to conclude that leaving out potentially scale forming divalent cations, such as Ba and Sr could lead to a misleading image of the initial wettability of the system.

Simulations and experiments performed by Fjelde et al. (2013a) show a strong indication that reducing the amount of divalent ions on the clay surface may be an important criteria for obtaining low salinity effect (LSE). Leaving out Ba and Sr may cause a unrepresentative prediction of the amount of divalent cations on the clay surface initially, as well as the amount of divalent cations being replaced.

2.10 – Investigating the effects of Ba and Sr

To investigate the effects of Ba and Sr being present in the FW simultions, using the PHREEQC modeling program has been run and compared with experimental results. Modeling of both saturation with FW and flooding was performed varying the concentrations of Ba and Sr in the FW. During the floodings, oil production and the effluents pH and ionic composition was monitored.

3 Simulations and PHREEQC

3.1– PHREEQC

PHREEQC version 2 is a computer program for simulating chemical reactions and transport processes in natural or polluted water (Parkhurst and Appelo, 1999). It is based on equilibrium chemistry of aqueous solutions interacting with minerals, gases, solid solutions, exchangers and sorption surfaces.

The system is capable of simulating a wide range of aqueous geochemical reactions including (Parkhust and Appelo 1999, Omekeh 2013):

- Mixing of waters
- Dissolution and precipitation of phases to achieve equilibrium with the aqueous phase
- Effect of changing temperature
- Ion exchange equilibria
- Surface complexion equilibria
- Advective transport modeling

Any number of solution compositions, solid solution, exchange or surface-complexation assemblages can be defined independently. PHREEQC is oriented toward a system equilibrium, rather than just aqueous equilibrium. It allows any combination of solution (or mixture of solutions), gas phase and assemblages to be brought together, any irreversible reaction can be added, and the resulting system to be brought to equilibrium. If kinetic reactions are defined, they are integrated with an automatic time-step algorithm, and system equilibrium is calculated after each time-step.

There are, however a number of limitations that need to be considered, as PHREEQC is only a general geochemical program (Parkhust and Appelo 1999):

- Ion-association and Debye Hückel expressions are used to account for the non-ideality of aqueous solutions. This works well for solutions with low ionic strength, but may not be as adequate in solutions with higher ionic strengths (SW and above). Some adjustments had been made to the Debye Hückel expressions

for the major ions, and the model may be reliable in sodium chloride dominated systems.

- The thermodynamic activity of an exchange species is assumed to be equal to its equivalent fraction in the ion-exchange model. In many field studies, ion-exchange modeling requires experimental data for reliable model application.
- Ideality is assumed when determining the activities for the components in a non-ideal, binary solid solution. This is usually an oversimplification.
- The model is not capable of detecting some physical impossibilities in the chemical system that is modeled.

3.2– Simulations

The main purpose of the simulations was to determine compositions for the synthetic brines to be used in the experimental study. The compositions selected were based on potential precipitation and amount of divalent ions adsorbed on the clay surfaces. According to Fjelde et al. (2013a), the LS brine selected for flooding should be the one ending up with the lowest concentration of divalent ions adsorbed. These simulations were done with brine/rock interactions only.

If Calcite mineral is present in the rock, the precipitation/dissolution of calcite is an important mechanism in a LSWF process. This is because it may significantly alter the composition of the injected brine. Another important mechanism affecting the composition of the injected brine is ion exchange. Both mechanisms will probably alter the composition of the injected brine. To get an accurate image of what is happening in the reservoir, it is important to look at the brine actually contacting the formation (Omekeh 2013, Fjelde et al. 2013a).

In the experiments, rock similar to the one used by Fjelde et al. (2013a) is flooded. To be able to compare the results, the LSW used should be similar to the ones used by them. They performed floodings using diluted FW, and LSW only containing KCl. These are therefore the two brines that were simulated when determining which LSW inject, and the one ending up with the lowest amount of divalent ions on the clay surface was chosen for the experiments.

As the saturation of the cores with FW where performed at room temperature the simulations for chossing the Ba and Sr concentrations in the initial formation brine, both room temperature and reservoir conditions were used. This was done because the precipitation of $BaCO_3$ and $SrCO_3$ are both temperature dependent reactions. Concentrations was chosen so

that there was no expectancy of precipitation at any part of either the preparation or flooding of the cores.

3.2.1 – Simulation Procedure

In the simulations run here, advective-trasport calculations were used to simulate advection and chemical reactions as the water moves through a 1D column. Based on IRIS experience on similar simulations, the column was divided into 20 cells with identifying numbers 1-20. Each cell contained a defined solution (the FW) numbered in the same way as the cells. Initially, all the cells contained the same brine, which was brought to equilibrium with the formation with defined composition. A second solution, solution 0 (the FW), was defined, and "injected" into the column by shifting solution 0 to cell 1, solution 1 to cell 2 and so on. 200 shifts where performed for each injected brine, equivalent to injecting 10 pore volumes (PV) of water. As the water "moved through" the column, cation exchange was integrated in each cell, while maintaining equilibrium with the solid-phase assemblage. When the injected brine was changed, the current cell solutions was saved, a new solution 0 composition (LSW) was defined, and a second series of 200 advection-transport calculations was performed.

The input parameters used in the simulations were:

- In-situ brine composition
- Injection brine composition (when determining FW composition, this composition was equal to the in-situ brine)
- Mineral composition of the rock
- CEC of the rock
- Dimensions of core plug

For each shift, the solution composition, the amount of ions on the clay surface, and the potential precipitation of $CaCO_3$, $BaCO_3$ and $SrCO_3$, as a result of the previous step, where monitored.

In this study simulations for choosing Ba and Sr concentrations in the saturating FW was run first, and then simulations for choosing which LSW composition to use for the floodings.

4 Experimental

Reservoir rock and stock tank oil (STO) from a sandstone oil reservoir in the North sea were used in the coreflooding experiments, performed at $80^{\circ}C$. FW samples from this oil reservoir were used to determine the composition of the synthetic formation water.

4.1– Brines

Compositions of the three synthetic formation brines (FW1, FW2 and FW3) and the low salinity brine (LSW-KCl) used are given in *Table 3*. FW1 is formation water without Ba and SO_4. FW2 is formation water with 3x the reported Sr concentration (~2200 ppm) and 15x original Ba concentration (~300ppm). FW3 is formation water with 3x Sr concentration and 1000x Ba concentration (~19000ppm).

Salt	FW1	FW2	FW3	LSW-KCl
NaCl	77.4	77.4	77.4	0
Na_2SO_4	0	0	0	0
$NaHCO_3$	0	0	0	0
KCl	0.42	0.42	0.42	0.0989
$MgCl_2*6H_2O$	3.55	3.55	3.55	0
$CaCl_2*2H_2O$	21.75	21.75	21.75	0
$SrCl_2*6H_2O$	2.25	6.75	6.75	0
BaCl2*$2H_2O$	0	0.53	34.93	0
LiCl	0	0	0	0

Table 3 - Compostitions of synthetic brines used

4.2– Crude Oil

The STO was prefiltered through a 0.45µm oil filter at 80℃ before it was used in the experiments.

4.3– Rock

The clay content of the core plugs was approximately 13wt%. The CEC of the rock was 2meq/100g and the clay fraction was mainly composed of illite, smectite, glauconite and chlorites.

4.4– Experimental Procedure

4.4.1 – Core Preparation

The reservoir core plugs were cleaned using cycles of toluene and methanol, before they were dried using N_2. One core was then saturated with FW1, one with FW2 and one with FW3, and absolute permeability was determined using multirates. Effluent samples of 5 PV where taken out. Using the unconfined porous disc method, the cores were drained to S_{wi} by gradually increasing the pressure of humidified nitrogen up to15 bar.

The cores were than mounted into tri-axial core holders, and an overburden pressure of 50 bars and a backpressure of 5 bars were established.

The nitrogen was then replaced by 3 PV of kerosene (mixture of Isopar H and toluene in a volume ratio 4:1) at a rate of 1 ml/min and the temperature was increased to 80℃. The kerosene was than replaced by 1.5 PV of a mixture of kerosene and STO (in the volume ratio 1:1) at a rate of 0.5 ml/min, before this mixture was replaced by 3 PV of STO also at a rate of 0.5 ml/min. The core plugs were aged for 7 days before another 2 PV of STO was injected. The core plugs were aged for another 7 days before $k_{ro}(S_{wi})$ was determined using multirates.

A sketch of the flooding set-up used is illustrated in *Figure 12*.

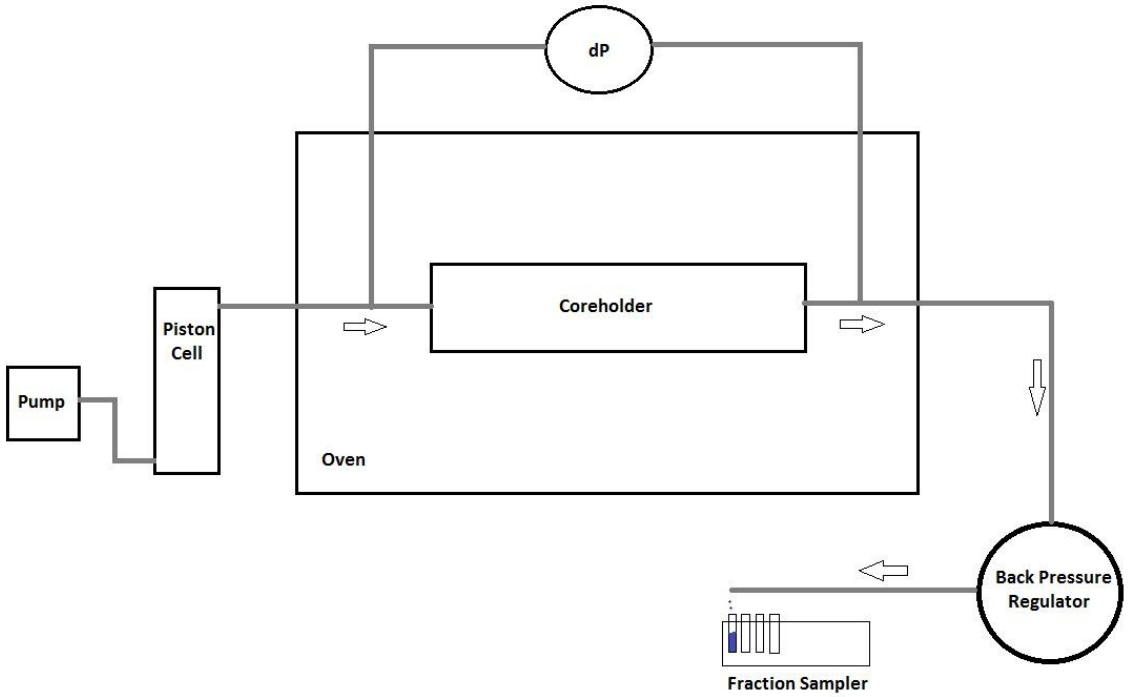

Figure 12 – Sketch of experimental flooding set up

4.4.2 – Flooding

After aging, the cores are first flooded with 10 PV of the same FW as they were saturated with, and then 10 PV of LSW-KCl. Both flooding steps are performed at a rate of 0.05 ml/min. Effluent samples of 5 ml were taken out. An overview of the floodings is shown in *Table 4*.

Experiment	Aging Brine	Flooding steps	Volume injected [PV]
1	FW1	FW1	10
		LSW-KCl	10
2	FW2	FW2	10
		LSW-KCl	10
3	FW3	FW3	10
		LSW-KCl	10

Table 4 - Overview of flooding experiments

4.4.3 – Analysis

The effluent samples taken out during the saturations where analysed for ionic composition using Inductive Coupled Plasma (ICP) and pH. The ICP analysis has an uncertainty of ± 15% for Ba, Ca, K, Mg, Na and S and ± 20% for Sr. The pH measurements have an uncertainty of ±0.01 after calibration.

During the flooding, pressure drop across the core (dP) was monitored.

The effluent samples were used to monitor oil production, water phase pH and ionic composition.

5 Results

5.1– Simulation Results

5.1.1 – Choice of brines

Saturation Brines

In the simulations run to choose FW compositions, the concentrations of Ba and Sr were varied. The main issue was to avoid precipitation, and to study the effect of Ba and Sr concentrations on the amount of divalent cations adsorbed on the clay surfaces. In the experimental study, the saturation with FW and the draining to S_{wi} on the unconfined porous plates was performed at room temperature, and the core flooding experiments where carried out at 80℃.. Therefore the simulations were run at both room temperature and 80℃ as the precipitation of $BaCO_3$ and $SrCO_3$ are both temperature dependent reactions.

The FW used by Fjelde et al. (2013a) contained Na_2SO_4. The first simulations showed that pretty much any concentration of both Ba and Sr would lead to precipitation of $BaSO_4$ and $SrSO_4$. It was therefore decided to remove the Na_2SO_4 from the FW. The composition of FW1 was the same as the FW used by Fjelde et al. (2013a), except Na_2SO_4 was removed. This composition was chosen to make sure that removing the Na_2SO_4 would not have any effect. See *Table 5*. (This is also the conclusion that can be drawn from the LSWF simulations, as the amount of ions on the clay surface was pretty much identical for the FW1 and the FW used by Fjelde et al. (2013a) (as shown in *Table 6*).

The elevated Sr concentration of ~2200ppm used in both FW2 and FW3 was chosen, as this was the highest possible concentration not leading to precipitation of $SrCO_3$ at any temperature.

Precipitation of $BaCO_3$ did not seem to be an issue here, as simulations with Ba concentration as high as~38000 ppm were run without the saturation index indicating any precipitation.

The Ba concentration in FW2 was chosen to be~300 ppm, as this is a typical concentration seen in North Sea petroleum sandstone reservoirs (Merdhah and Yassin 2007). The Ba concentration in FW3 of ~19000 ppm was chosen to get an "extreme" example of the potential effects.

The saturation simulations were run with the assumption that FW was already in the core, and in equilibrium with the formation. The solution/effluent concentrations and the amount of the different ions present on the clay surface during the simulated flooding with FW therefore remained at about a constant level. The simulations were therefore not able to show the actual reactions that took place in the experiment when air was replaced with FW. For this reason the effluent profiles from the simulations are not presented here.

The amount of the different ions that were adsorbed on the clay surface in the FW saturated cores are shown in *Table 5*. X represents the exchange site the ion was adsorbed to. The results for FW1 and FW** (FW used by Fjelde et al. (2013a)) indicated that removing the Na_2SO_4 will not have any effect on the ion exchange. The results for FW2 indicate that increasing the concentration of Ba and Sr will slightly increase the amount of divalent ions on the clay surface and hence reduce the amount of monovalent ions. The results for FW3 indicate that a large increase in Ba will have a significant effect on the amount of adsorbed divalent ions. The amount of divalent ions adsorbed was increased by 34 % compared with FW2, and by 43% compared to FW1.

	FW1	FW2	FW3	FW**
NaX [moles]	0.1274	0.1232	0.0985	0.1274
KX [moles]	0.0065	0.0063	0.0053	0.0065
CaX2 [moles]	0.0324	0.0303	0.0221	0.0324
MgX2 [moles]	$3.8 \cdot 10^{-5}$	$3.5 \cdot 10^{-5}$	$2.2 \cdot 10^{-5}$	$3.8 \cdot 10^{-5}$
BaX2 [moles]	0	0.0005	0.0231	0
SrX2 [moles]	0.0021	0.0060	0.0044	0.0021
Divalent [moles]	0.0345	0.0368	0.0495	0.0345
Monovalent [moles]	0.1339	0.1295	0.1039	0.1339

** Composition of FW used by Fjelde et al. (2013a)

Table 5 - Amount of ions retained on clay surfaces after saturation with different formation waters. X represents the exchange site the ion is adsorbed to.

Flooding brines

LSW composition was selected based on simulation evaluating the same LS brines as used by Fjelde et al. (2013a). They used FW diluted 1000x, and LS brine only containing KCl. The brine that should be used is the one leading to the lowest concentration of divalent cations on the clay surface. The amounts of the different ions on the clay surfaces given by the simulations are shown in *Table 6*. All the simulations indicated that flooding with LS brine only containing KCl would lead to the lowest concentrations of divalent ions, and hence this brine was chosen for the flooding experiments.

Saturation brine:	FW1		FW2		FW3		FW**	
Flooding brine:	**LSW-KCl**	**LSW2***	**LSW-KCl**	**LSW2***	**LSW-KCl**	**LSW2**	**LSW-KCl**	**LSW2***
NaX [moles]	0.0711	0.0632	0.0681	0.0589	0.0513	0.0342	0.0711	0.0632
KX [moles]	0.0027	0.0024	0.0026	0.0022	0.0019	0.0013	0.0027	0.0024
CaX2 [moles]	0.0669	0.0700	0.0645	0.0663	0.0501	0.0511	0.06690	0.0700
MgX2 [moles]	$7.0 \cdot 10^{-6}$	$5.5 \cdot 10^{-6}$	$6.4 \cdot 10^{-6}$	$4.8 \cdot 10^{-6}$	$3.6 \cdot 10^{-6}$	$1.7 \cdot 10^{-6}$	$7.0 \cdot 10^{-6}$	$5.5 \cdot 10^{-6}$
BaX2 [moles]	0	0	0.0004	0.0006	0.0243	0.0294	0	0
SrX2 [moles]	0.0018	0.0028	0.0054	0.0078	0.0045	0.0074	0.0018	0.0028
Divalent [moles]	0.0687	0.0798	0.0703	0.0747	0.0790	0.0879	0.0687	0.0798
Monovalent [moles]	0.0737	0.0655	0.0707	0.0611	0.0532	0.0355	0.0737	0.0655

*The FW used for saturation diluted 1000x

Table 6 – Simulated amounts of ions on the clay surface in cell 20 after flooding a FW saturated formation with 10 PV of low salinity brine.

5.1.2 – Flooding simulations

In the flooding simulation, the amount of ions retained on the clay surfaces after 10 PV of FW has been injected was approximately equal to the values given in *Table 5*. This was due to the oil not being present in the simulations, and because of the assumption that the core was already saturated with a brine of similar composition as the one used for flooding.

When LSW-KCl was injected, the concentrations of the different ions varied through the formation. The concentrations of ions on the clay surfaces after 10PV of LSW-KCl had been injected are given in *Table 7*. Similar for all the cores were that the total amount of divalent ions adsorbed seem to increase when LSW-KCl was injected. In all the simulations, the amount of Na adsorbed was reduced in all the cells. This was probably due to the clays having the least affinity towards Na (IDS 1982, Suarez and Zahow 1989, Bennet 2013). When concentration of Na in the brine contacting the formation was reduced, other ions were preferred.

K concentration was, as expected, increased in the first cells in Simulation 1 and 2, but as water moved through the formation, the amount of K adsorbed was reduced. This was probably due to the K concentration being so low, that the released ions, that were either replaced by K or released by dissolution in the first cells, will be preferred over K by the formation in the later cells. Hence K, and also Na was released. In Simulation 3, the increase in K adsorbed in the first cells was not seen, and the amount of K adsorbed was reduced in the entire core.

In Simulation 1 and 2 the amount of Ca adsorbed in the first cell seemed to return to approximately the same value as after flooding with FW1. See *Table 7*. In the later cells however, the amount of Ca adsorbed was significantly increased. This was probably due to the precipitation of calcite and further Ca being "preferred" by the formation. In Simulation 3, the increase in Ca concentration adsorbed was largest in the first cell, and then smaller and smaller later in the formation.

The amount of Mg adsorbed was significantly increased in the first cell of both Simulation 1 and 2. In the later cells however, the Mg concentration was reduced to a lower value than after flooding with FW. In Simulation 3, the amount of Mg adsorbed was reduced through the entire formation indicating that Mg was released.

As seen in *Table 6*, the amount of Sr adsorbed remained the same throughout the entire flooding in both Simulation 1 and 2. In Simulation 3, some Sr was released from the first cells, but in the last half of the core, the amount for Sr adsorbed remained constant.

Ba did not seem to whether be released or retained in simulations 1 and 2. The amounts adsorbed remained the same throughout the floodings. In Simulation 3 the amount of Ba adsorbed was reduced in the first cells indicating that some Ba was being released.

Saturation brine	**FW1 (Simulation 1)**			**FW2 (Simulation 2)**			**FW3 (Simulation 3)**		
Dimensionless distance:	**0**	**0.5**	**1**	**0**	**0.5**	**1**	**0**	**0.5**	**1**
NaX [moles]:	0.023	0.060	0.096	0.021	0.055	0.091	0.021	0.043	0.069
KX [moles]:	0.015	0.002	0.004	0.014	0.002	0.003	0.001	0.002	0.003
CaX2 [moles]:	0.033	0.068	0.050	0.031	0.066	0.050	0.068	0.052	0.038
MgX2 [moles]:	0.047	$5.1 \cdot 10^{-6}$	$1.3 \cdot 10^{-5}$	0.047	$4.3 \cdot 10^{-6}$	$1.9 \cdot 10^{-5}$	$6.3 \cdot 10^{-6}$	$2.6 \cdot 10^{-6}$	$6.7 \cdot 10^{-6}$
SrX2 [moles]:	0.022	0.002	0.002	0.006	0.006	0.006	0.0035	0.0044	0.0044
BaX2 [moles]:	0	0	0	$5 \cdot 10^{-4}$	$5 \cdot 10^{-4}$	$5 \cdot 10^{-4}$	0.018	0.023	0.023
Monovalent [moles]:	0.038	0.062	0.099	0.035	0.057	0.094	0.022	0.044	0.071
Divalent [moles]:	0.102	0.071	0.052	0.084	0.073	0.054	0.095	0.079	0.066

Table 7 - Concentrations of different ions present on the clay surfaces after flooding with 10PV of FW and than 10PV of LSW-KCl. The concentrations are given at dimensionless distance 0, 0.5 and 1 representing cells 1, 10 and 20 respectively.

5.2– Experimental Results

5.2.1 – Fluid Properties and Core Data

Viscosities of the fluids in the core flooding experiments (at 80℃) are given in *Table 8* and the properties of the three composite cores are given in *Table 9*.

	FW1	FW2	FW3	LSW-KCl	STO
Viscocity [cP]	0.419	0.421	0.446	0.355	1.5

Table 8 – Fluid viscocities at 80℃

Core no	Lenght [cm]	Diameter [cm]	Kabs [mD]	PV [ml]	Φ [fraction]	S_{wi} [fraction PV]
1	7.989	3.735	95.92	21.99	0.25*	0.25
2	7.810	3.740	90.80	21.54	0.25*	0.28
3	7.810	3.740	92,46	21.62	0.25*	0.32

** assumed based on IRIS experience for same reservoir rock (Fjelde, 2013b)*

Table 9 - Properties of the composite cores used in the flooding experiment

5.2.2 – Saturation of the cores with different FW

The ionic composition of the effluent samples taken during saturation of Core1, Core2 and Core3 with FW are given in *Figure 13*, *Figure 14* and Figure 15 successively. Increased concentration of K initially was seen in all the floodings. This may be due to contamination of the rock during drilling of the well with KCl mud (Fjelde 2013b)

The results showed that the ionic composition of the FW affected the reactions with the formation. Saturating Core1 with FW containing no Ba and only low concentrations of Sr (FW1), showed a high release of Mg in the beginning, while Ca concentration remained approximately at injected level. See *Figure 13*. At the same time the concentration of Na and Sr were reduced initially, indicating that these ions were adsorbed on the clay surface. The formation also seemed to release some Ba when the other concentrations were pretty much stabilized. This release of Ba was still going on when the saturation of Core1 was ended, indicating that the formation was not yet in equilibrium with FW1. Core1 was flooded with a lower number of PVs compared to the other two cores due to rate delivering problems with the pump used.

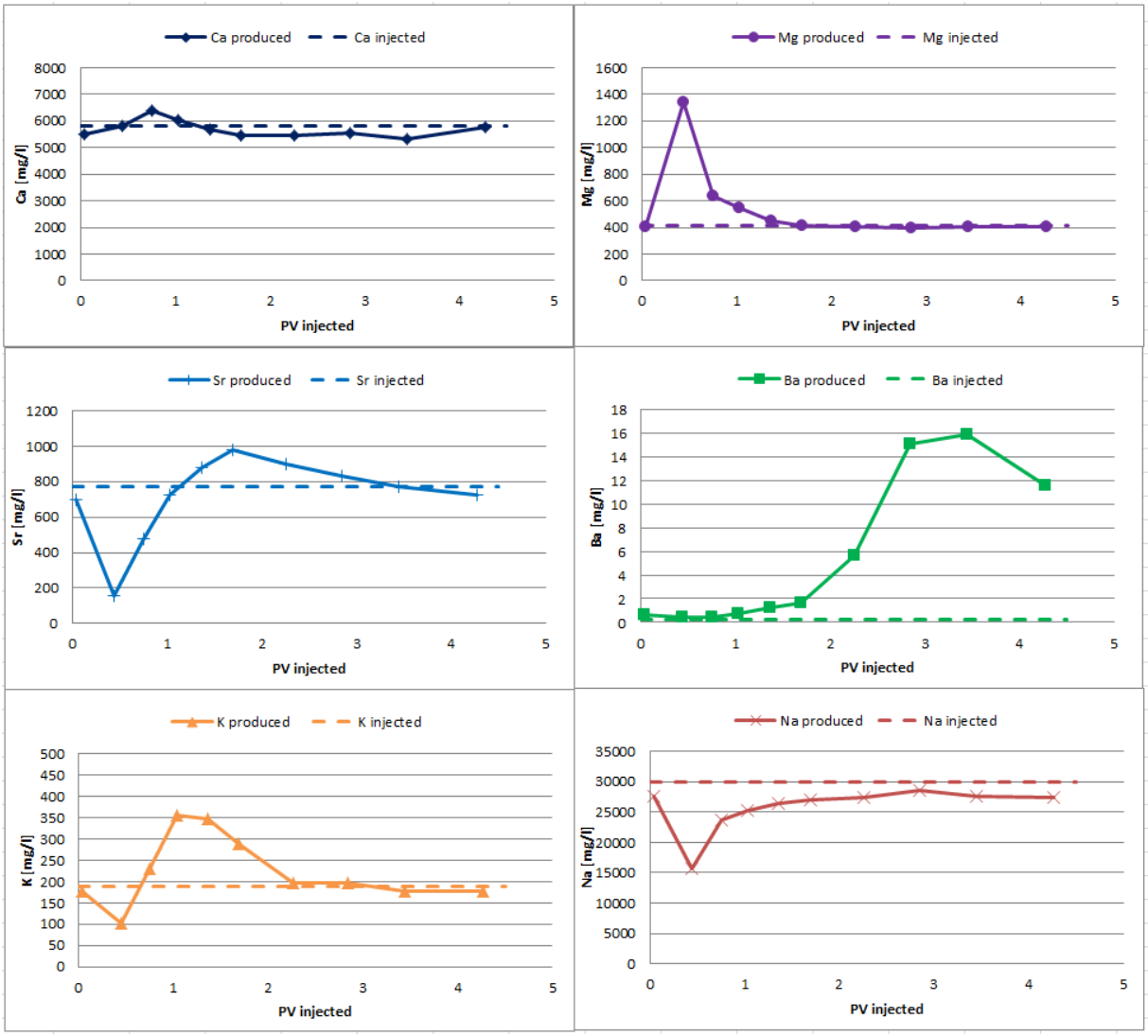

Figure 13 - Ionic compostition of effluents during saturation of Core1 with FW1

As shown in *Figure 14*, increasing the concentration of Ba and Sr (FW2) caused higher adsorption of the monovalent ions (Na and K). The amount of Ca released was increased, but the amount of both Mg and Sr released was reduced. Both Ba and Sr were adsorbed initially before the effluent concentration stabilized at approximately injected level (The difference between the produced and injected level is within the uncertainty level of the ICP analysis (±15%)).

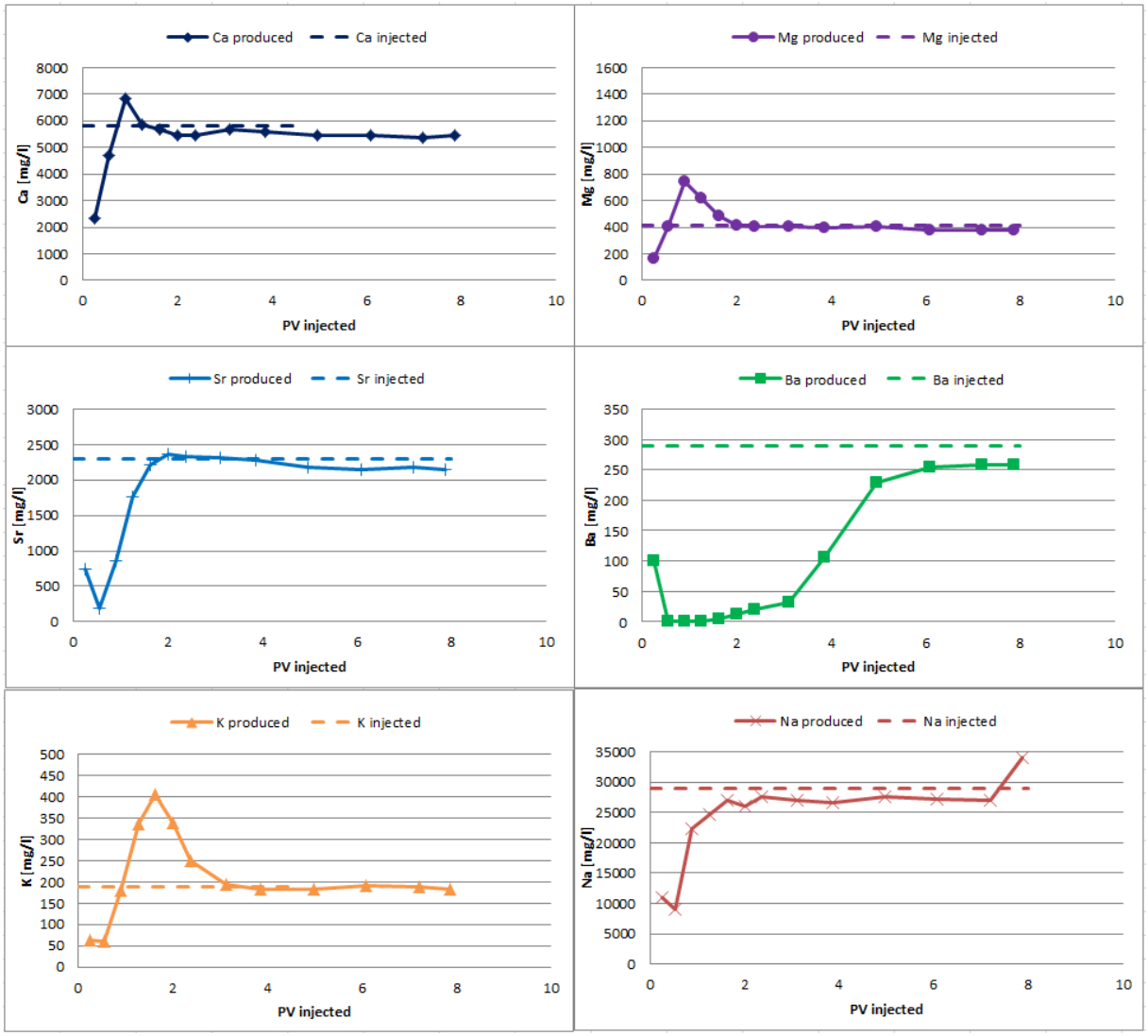

Figure 14 - Ionic compostition of effluents during saturation of Core2 with FW2

Increasing the Ba concentration even more (FW3) reduced the adsorption of monovalent ions significantly. See Figure 15. The amount of Na in the effluents was approximately constant throughout the flooding. The amount of Ca released was increased, while the amount of Mg released was reduced. Also, the adsorption of Sr was significantly reduced, indicating that the Ba ions may be preferred over Sr at some of the adsorptions sites on the clay due to higher affinity (IDS 1982, Suarez and Zahow 1989, Bennet 2013).

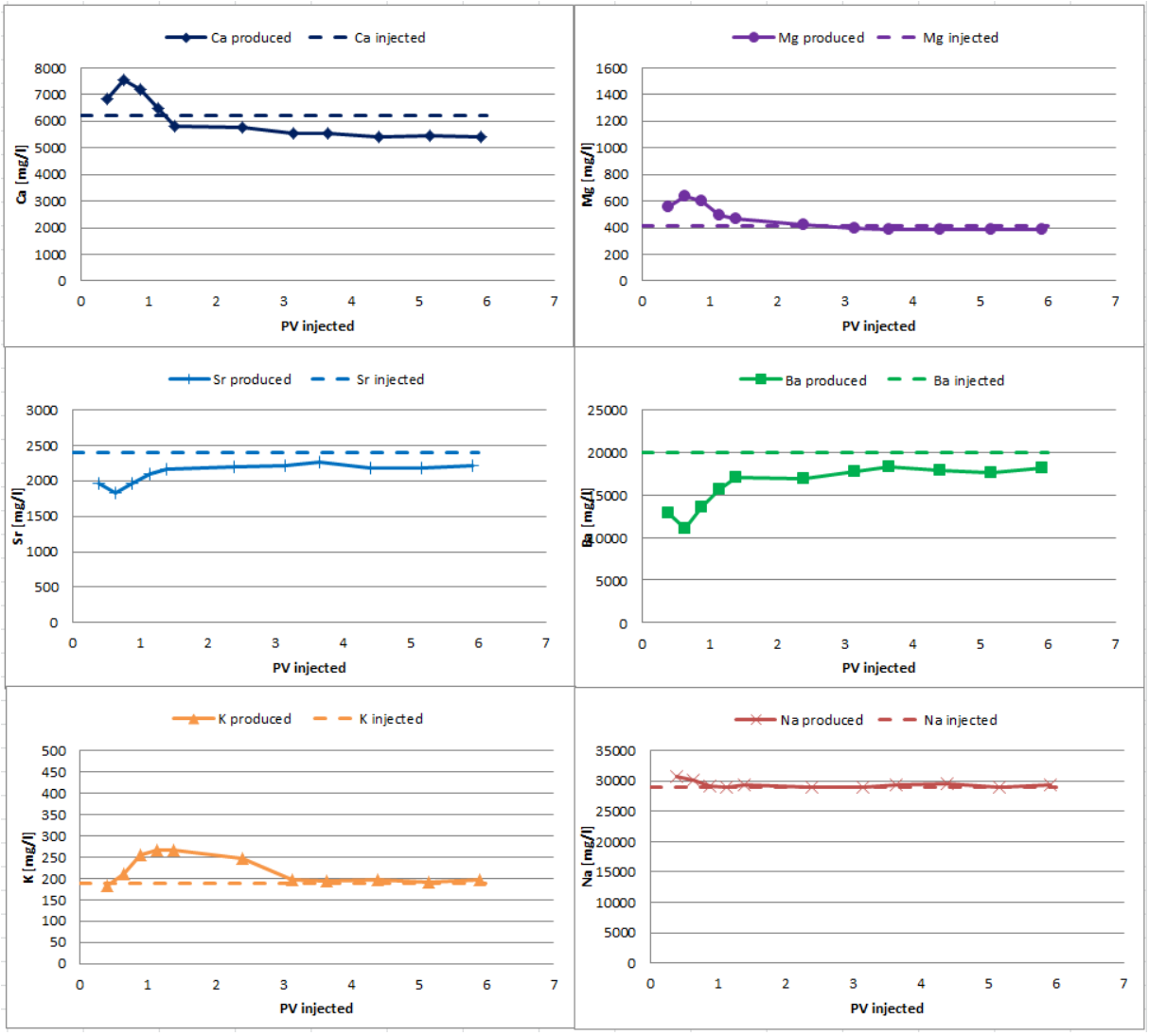

Figure 15 - *Ionic compostition of effluents during saturation of Core3 with FW3*

5.2.3 Oil Production Differential Pressure across the Core and Relative Permeabilities

End point relative permeabilities and residual oil saturation (S_{or}) after each flooding step is given in *Table 10* and the oil saturation and dP for the flooding experiments are given in *Figure 16*, *Figure 19* and *Figure 21* successively. For comparison, S_o and dP plot from Experiment 1 performed by Fjelde et al. (2012) is shown in *Figure 17* (Flooding with FW – sea water – FW diluted 100x – FW diluted 1000x).

Core No	**Aging Brine**	S_{wi}	$k_{ro}(S_{wi})$	**Flooding steps**	S_{or}	$k_{rw}(S_{or})$
1	FW1	0.25	0.71	FW1	(0.37)	0.087
				LSW-KCl	(0.30)	0.14
2	FW2	0.28	0.83	FW2	0.42	0.093
				LSW-KCl	0.32	0.18
3	FW3	0.32	0.81	FW3	0.29	0.084
				LSW-KCl	0.26	0.10

Table 10 – End point relative permeabilities and residual oil saturation after each flooding step

When FW1 was injected into Core 1, most of the oil was produced before the water breakthrough, and the dP seemed to settle at a stable level until about 6 PV of brine had been injected. See *Figure 16*. k_{rw} after 6 PV was 0.092 (determined by injection rate of 0.05 ml/min). The following pressure buildup shown was probably caused by blockage in the flooding rig. There was a drop in pressure right before the FW injection was ended, and the 0.5 ml of STO produced immediately after starting LSW-KCl injection came from the dead volume (DV) of the rig and was hence produced during the FW injection. After LSW-KCl had been injected, a bypass flooding of the rig at high rate was performed. This resulted in an additional production of about 1.8 ml of STO. A permeability measurement of Core1 using multirate was then performed, showing that the permeability of the core had not been significantly reduced. See *Figure 16*. Unfortunately, it was not possible to know the exact

production period during LSW-KCl, and hence it is difficult to evaluate the wettability of the system.

The results from Experiment 1 presented by Fjelde et al. (2013a) showed faster production during FW injection than Core1 in the present study. The S_{or} reached by Fjelde et al. (2013a) was also significantly lower. The relative permeability results presented by Fjelde et al.(2013a) (see *Figure 18*) show higher $k_{ro}(S_{wi})$ and lower $k_{rw}(S_{or})$ than Core1. This all indicates that removing SO_4 from the FW causes the core to become less water wet.

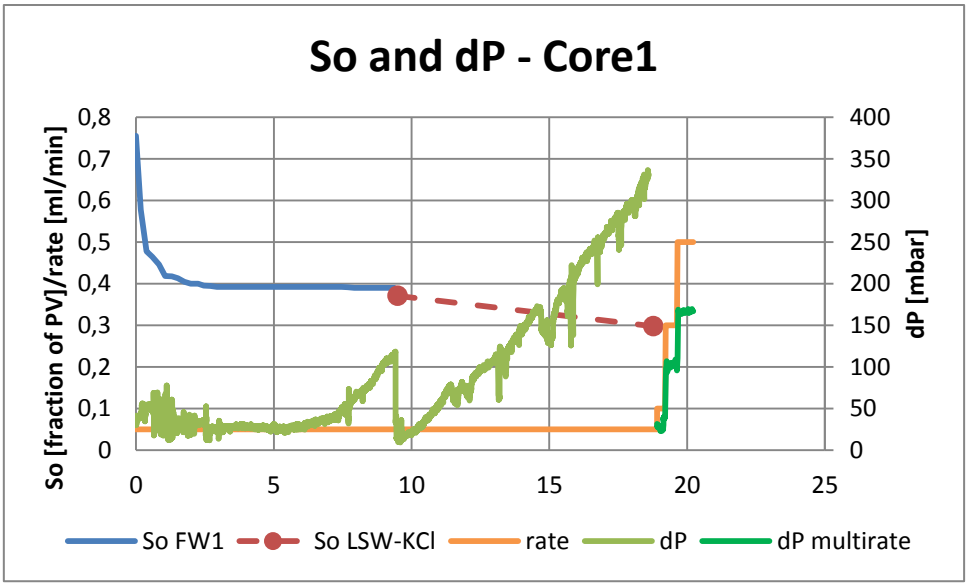

Figure 16 - Oil saturation, dP and flooding rate during flooding of Core1. Red line is dashed due to unknown production profile.

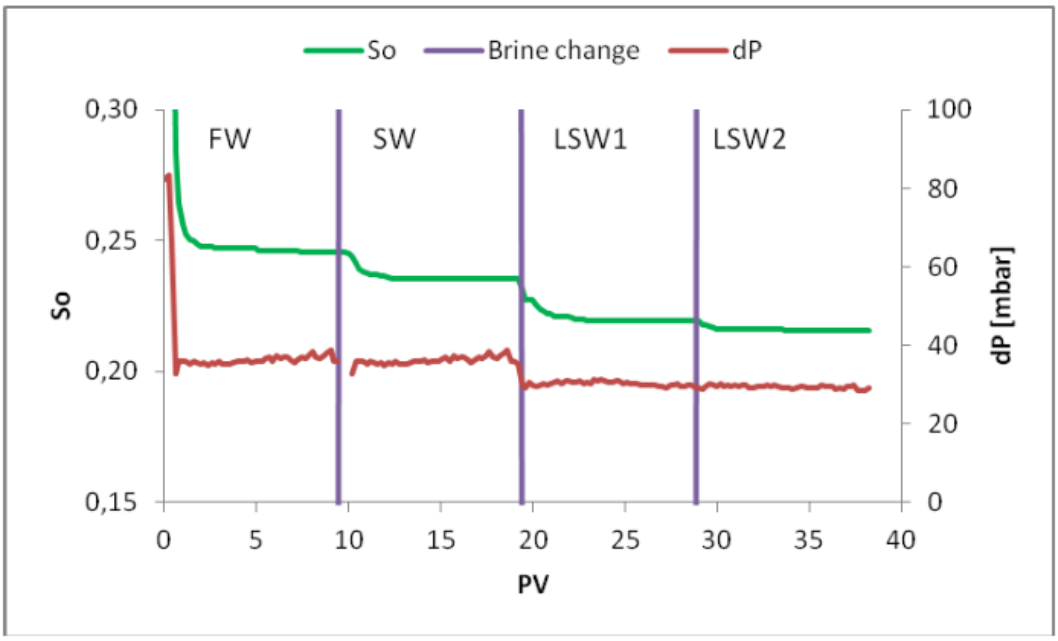

Figure 17 - Oil saturation and dP Experiment1 Fjelde et al. (2012)

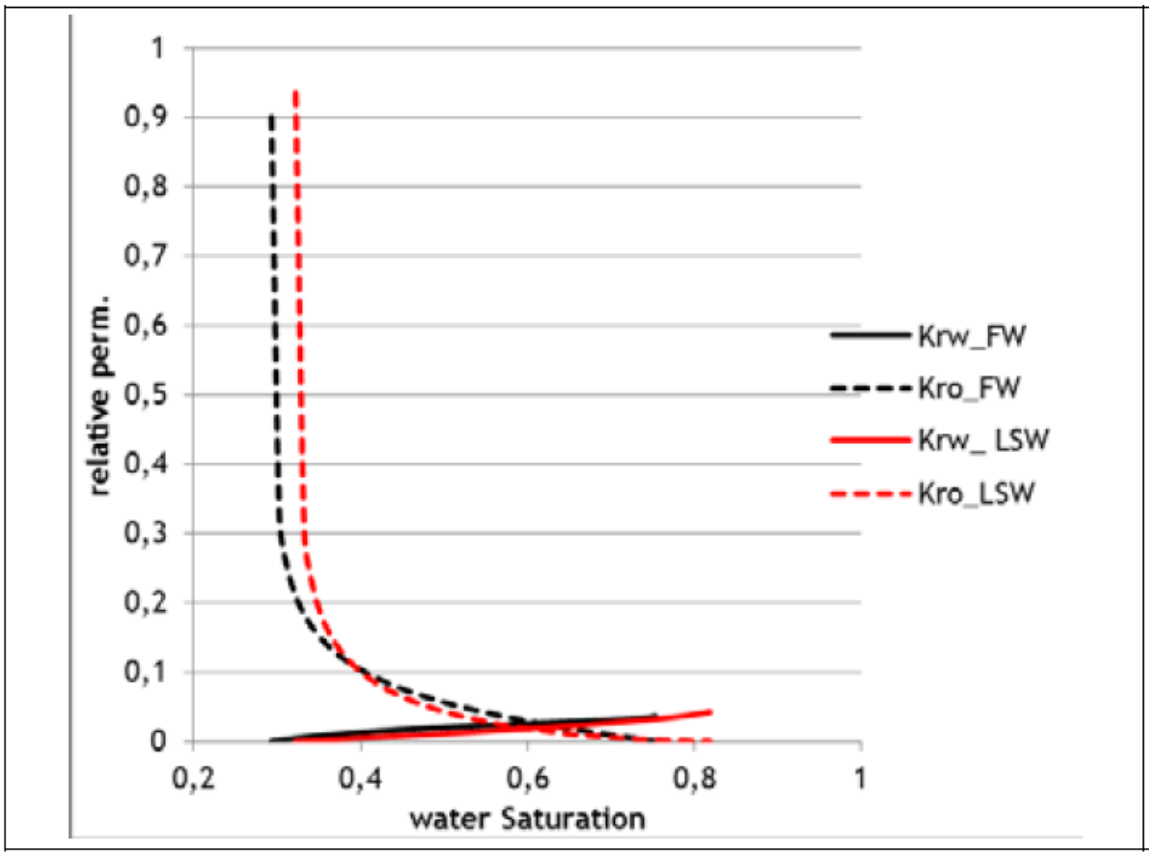

Figure 18 - Estimated relative permeability curves from Experiment 1 presented by Fjelde et al. (2012)

As shown in *Figure 19*, initial production during FW2 injection to Core2 was a slightly faster than during FW1 injection in Core1. However, the S_{or} reached in Core2 was higher than in Core1, which indicates a more water wet system. This was also confirmed by the relative permeabilities showing a significantly higher $k_{ro}(S_{wi})$ for Core2. Injecting the LSW-KCl brine to Core2 caused a significant decrease in S_{or}. However, the production was slow, and more PV should probably have been injected as it appeared that the core had not reached equilibrium when the injection was ended. As STO was produced during LSW-KCl, dP did not decrease as expected. The effluent concentration of S from Core2 had an increase during injection of LSW-KCl effluents from the two other cores did't have. In the ICP analysis, S detected could be SO_4^{2-}, S^- and HS^-. If the elevated S concentration was due to an elevated SO_4^{2-} concentration, the pressure increase might be due to precipitation of $BaSO_4$ and/or $SrSO_4$. See *Figure 20*. This might cause the permeability to decrease, and hence the dP to increase. The increase in S concentration was also seen in the effluents from the two other cores but to a much smaller degree.

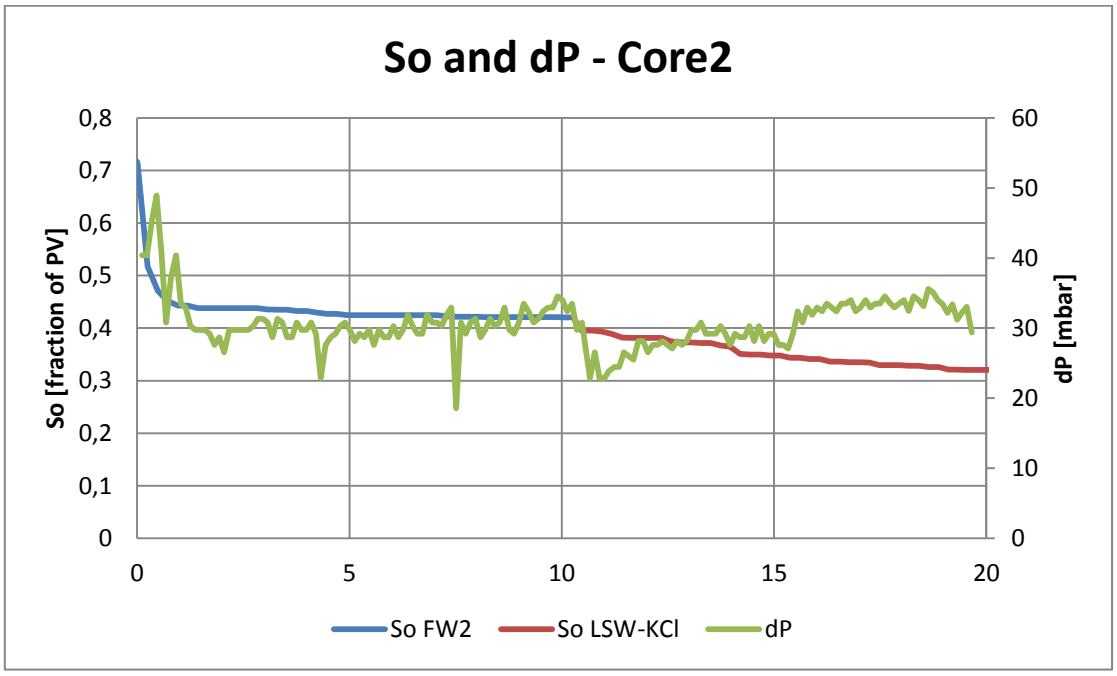

Figure 19 - Oil saturation and dP during flooding of Core2

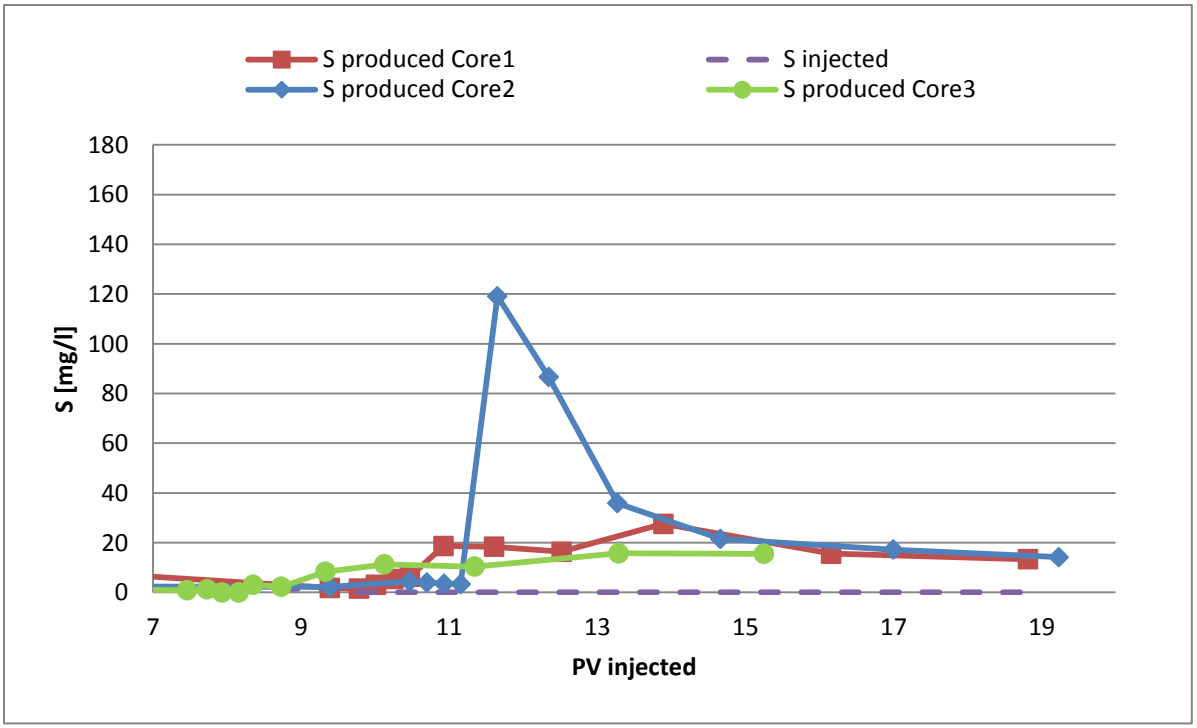

Figure 20 - Effluent S concentrations during LSW-KCl flooding from all three cores.

When FW3 was injected into Core3, most of the oil was produced almost immediately. See *Figure 21*. Also the S_{or} reached was lower than for the two other cores. The relative permeability values for the FW3 flooding were similar to the ones in Core2. Similar k_{rw} value, at a lower S_{or} combined with the oil being produced faster indicate that the extreme Ba concentration caused Core3 to become more water wet than Core2. When injecting LSW-KCl in Core3 a small amount of oil was slowly produced. The amount produced during the LS step was however much smaller than for Core1 and 2. This was also confirmed by a smaller change in k_{rw} than for the two other cores. The logging of the dP failed, and only manual recordings are available for Core3. However, the dP seem to remain rather constant through the LSW-KCl flooding.

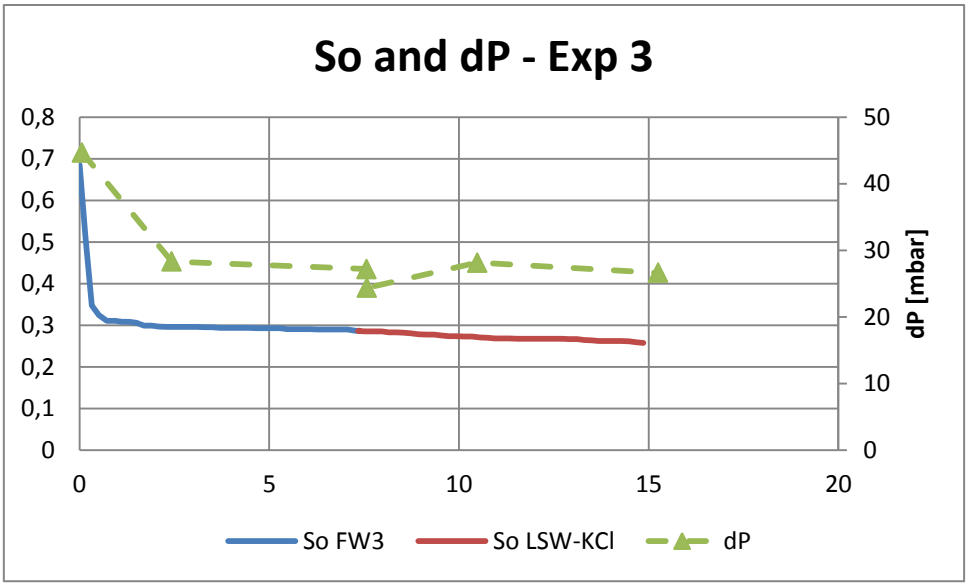

Figure 21 - Oil saturation and dP during flooding of Core3

5.2.4 – pH

When FW1 was injected in Experiment 1, the effluent pH was higher than the injection level as shown in *Figure 22*. This indicates a reaction between the formation and the injected brine. When the LSW-KCl was injected, the pH of the effluent increased even more. According to Omekeh et al. 2012, this pH increase was probably due dissolution of calcite during FW injection which causes the pH to remain low. As the LSW was injected, the dissolution of calcite is smaller causing the pH to rise. The pH results were similar to the ones reported by Fjelde et al. (2012) for injection of FW – SW – FW diluted 100x and FW diluted 1000x. and LSW-KCl (shown in *Figure 23* and *Figure 24*) indicating that removing SO_4^{2-} will not have an effect on the pH.

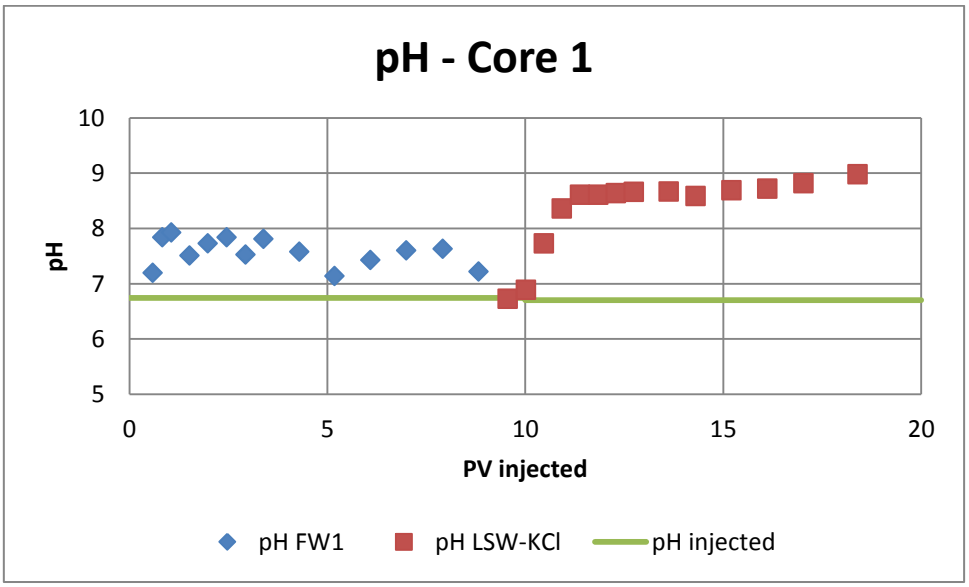

Figure 22 - Effluent pH during injection of FW1 and LSW-KCl to Core 1

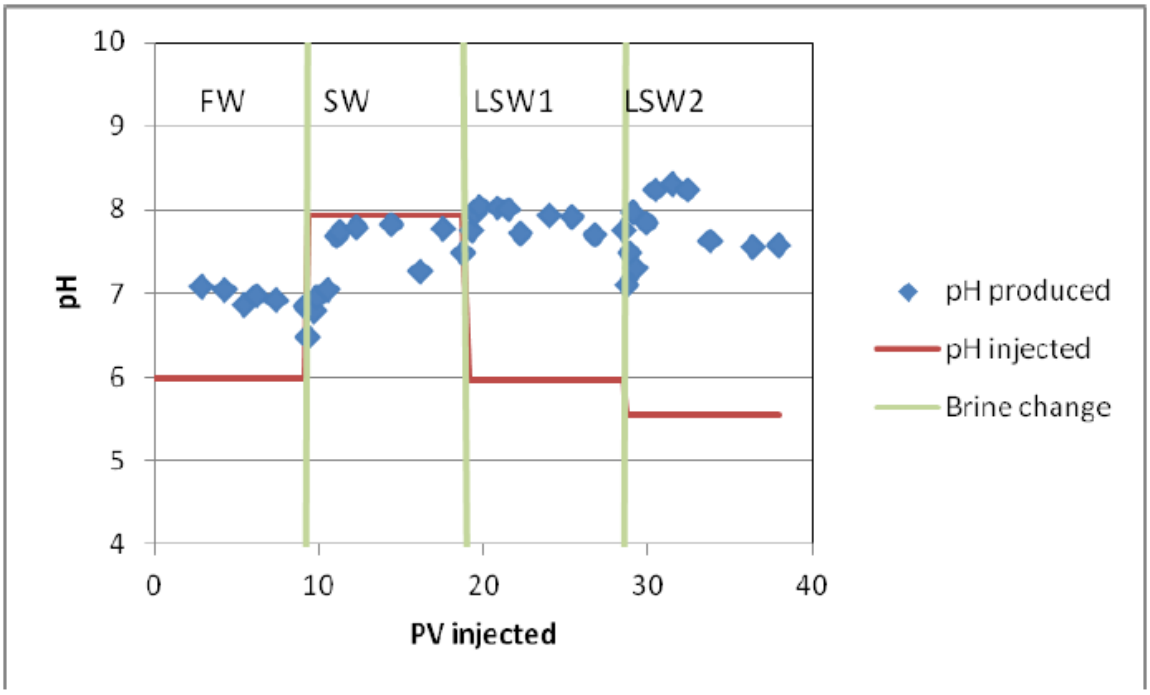

Figure 23 – pH from Experiment1 – core flooded with FW – SW – FW diluted 100x – FW diluted 1000x (Fjelde et al. 2012)

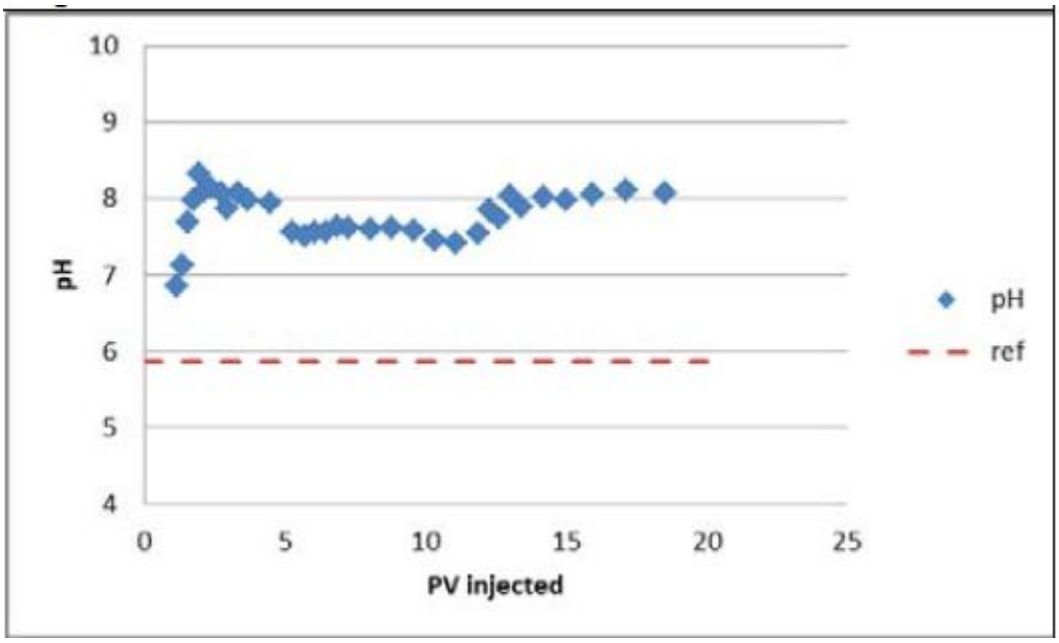

Figure 24 - pH from Experiment 4 – core flooded with LSW-KCl only (Fjelde et al. 2013a)

When FW2 was injected in Experiment 2, the effluent pH seems to stay at approximately the same value as injected. See *Figure 25*. When LSW-KCl was injected, the effluent pH rose to a higher value than injected, indicating a reaction between the injected brine and the formation. The rise in pH was similar to the one seen in Core1.

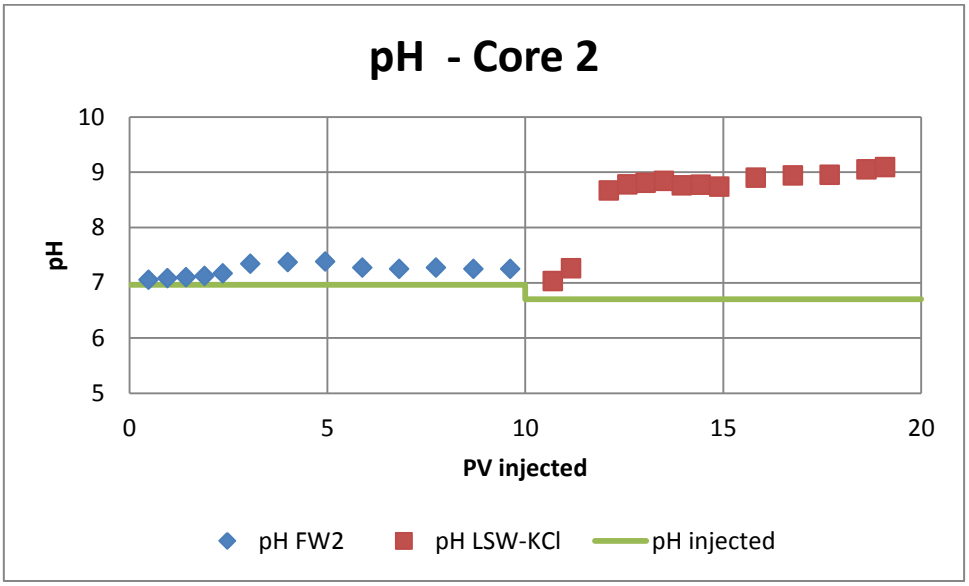

Figure 25 - Effluent pH during injection of FW2 and LSW-KCl to Core 2

When FW3 was injected in Experiment 3, the pH of the effluent remained at approximately the same value as injected as shown in *Figure 26*. When the LSW-KCl was injected, the pH of the effluent rose to a higher value than injected, indicating a reaction between the injected brine and the formation. The pH rose to approximately the same level during LSWF in all the three cores, but to a higher level than obtained by Fjelde et al. (2013a) both when changing from FW to LSW (SW injected in between), as shown in *Figure 23*, and also when flooding with LSW-KCl only as shown in *Figure 24*.

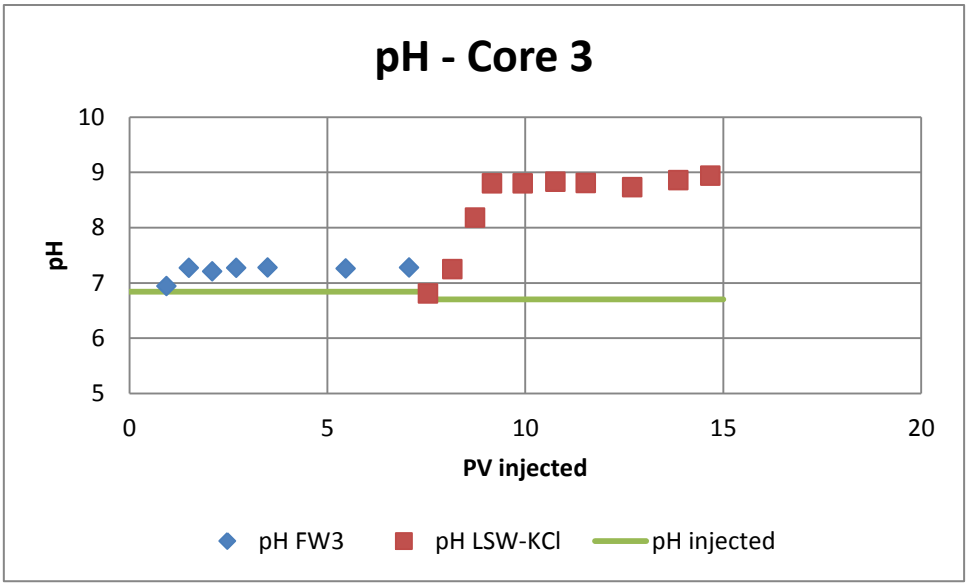

Figure 26 - Effluent pH during injection of FW3 and LSW-Kcl to Core 3

5.2.5 – Ionic Composition of effluents

The saturation floodings and drainage to S_{wi} on unconfined porous plates where performed at room temperature. The corefloodings where performed at 80℃, and the cores not being in equilibrium with the different FWs at the start of the FW floodings might be due to reactions caused by the temperature increase.

Core1:

Effluent ionic compositions from Core1 floodings are shown in *Figure 27* (Ca, Mg, K and Na) and *Figure 28* (Ba and Sr). Figures on the left show both FW1 and LSW-KCl injection, while the figures on the right give a closer look at the LSW-KCl injection. The results from the FW1 effluents show that very large amounts of all the ions were adsorbed. This could be due to injection of smaller FW volume due to pump failure, but as it seemed that all the ions (except for Ba) had reached injected level, it seems unlikely that that much retention should take place. Also, the shapes of the graphs are fairly similar, which might indicate measurement errors. The FW1 effluent results will therefore not be used for further interpretation. However, the concentrations in the last measurement points seem to have reached injected level, and effluent concentrations from the LSW-KCl injection are interpreted.

When LSW-KCl was injected, Ca concentration remained above injected level indicating that Ca was being released from the formation, as seen in *Figure 27*. Mg concentration also remained above injected level until the end of the LSW-KCl injection. As shown by *Figure 27*, the Na concentration remained above injected level through the entire injection, indicating that Na was being released. The K concentration was lower than injected all through the LSW-KCl injection. K was being retained by the formation, replacing Na, Ca, and Mg. This ion exchange was also seen in Experiment 4 performed by Fjelde et al. (2013a) where only LSW-KCl was injected. See *Figure 30*.

As shown in *Figure 28*. The concentration of Ba was quickly reduced and stabilized at injected level when LSW-KCl was injected. This indicates that most of the Ba present in the formation initially was released during FW1 injection. When LSW-KCl was injected some Sr was released before the concentration was reduced to injected level.

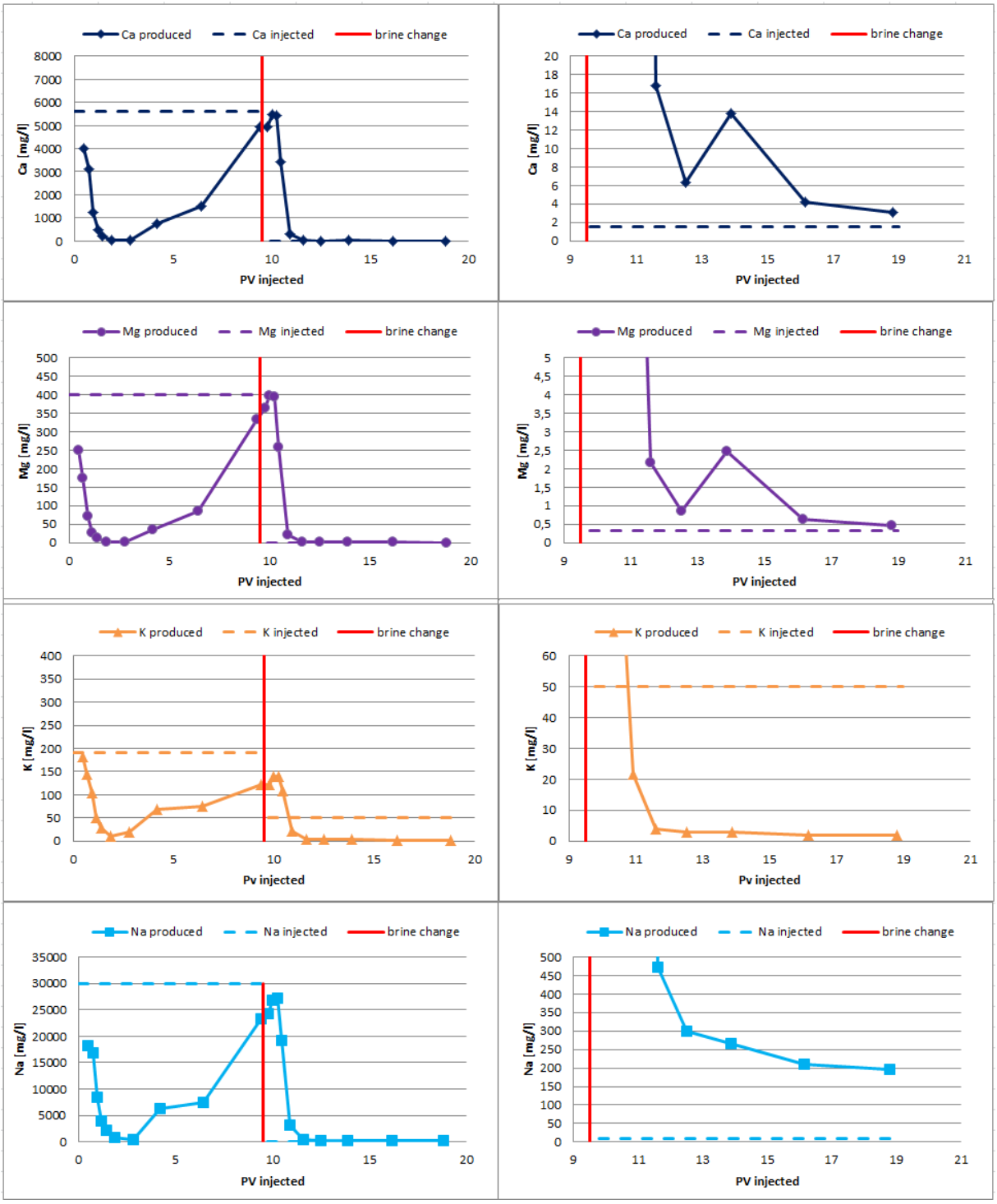

Figure 27 - Effluent concentrations of Ca, Mg, K and Na from Core1. Figures on the left show both FW1 and LSW-KCl injection, while figures on the right show LSW-KCl injection only

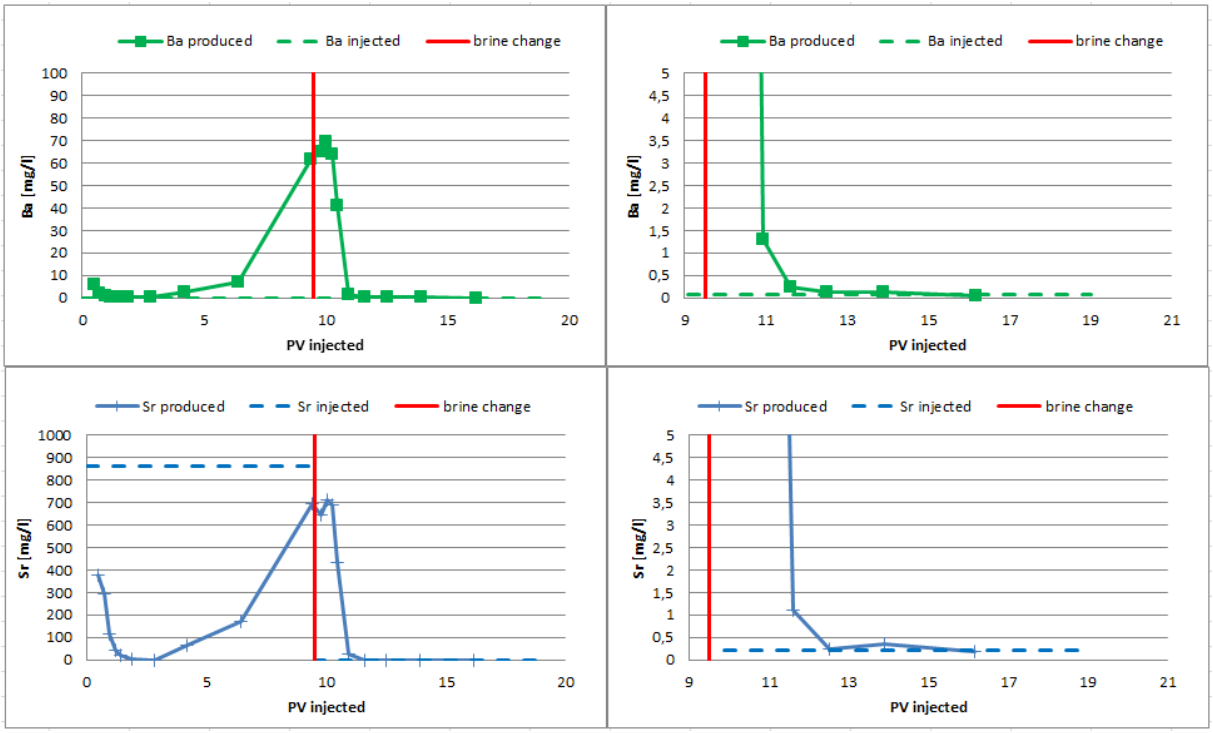

Figure 28 - Effluent concentrations of Ba and Sr from Core1. Figures on the left show both FW1 and LSW-KCl injection, while figures on the right show LSW-KCl injection only

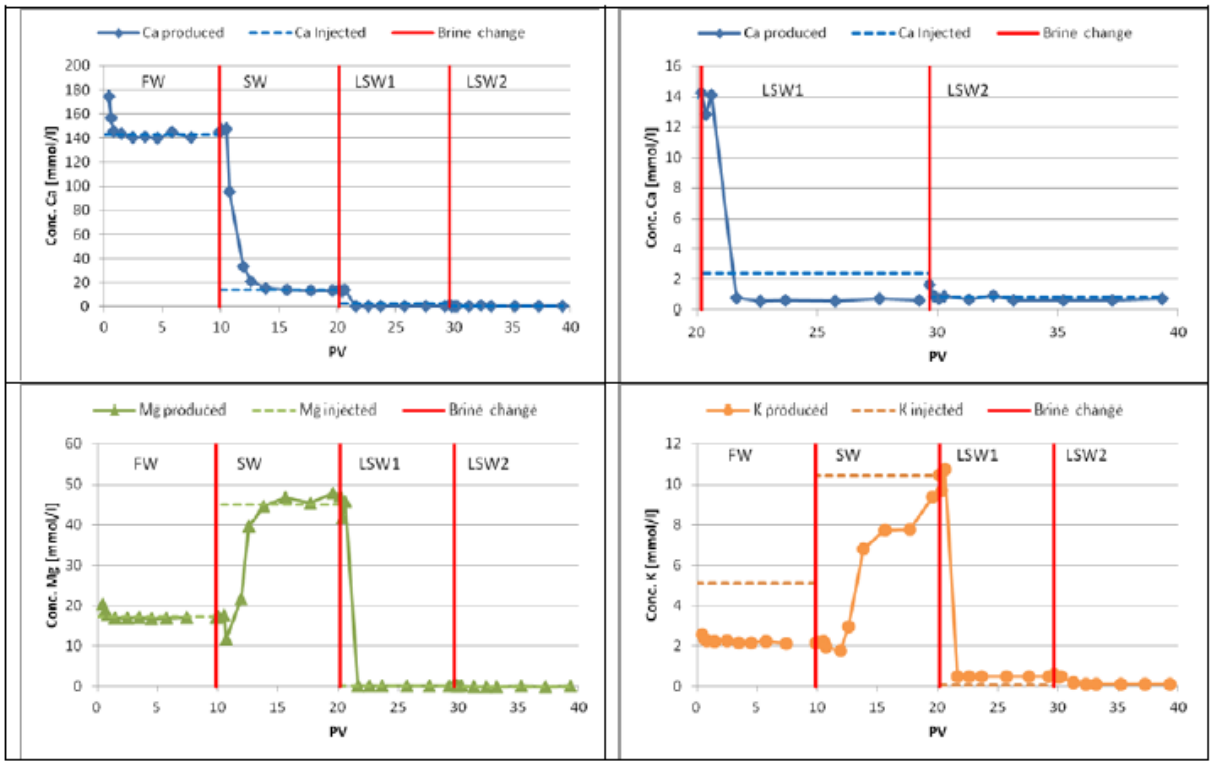

Figure 29 - Ionic comporition of Experiment 1 performed by Fjelde et.al (2012). Core was flooded with FW – SW – FW diluted 100x – FW diluted 1000x.

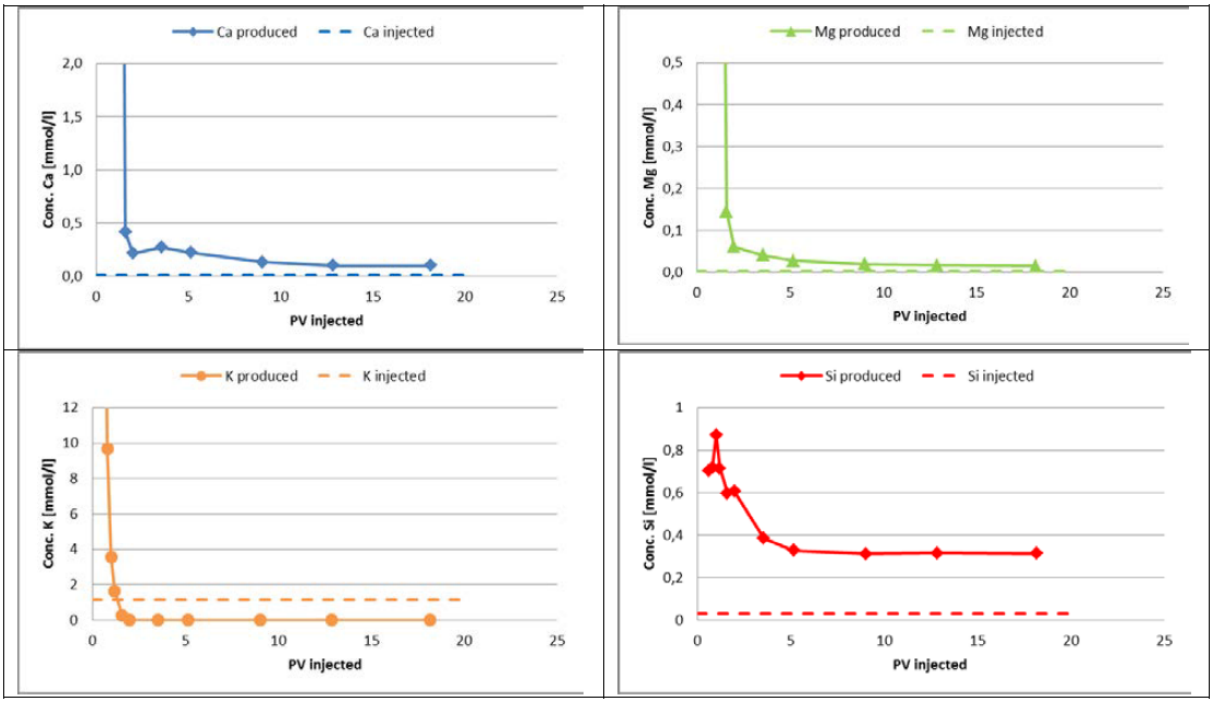

Figure 30 - Ionic composition of Experiment 4 performed by Fjelde et al. (2013a). Core is flooded with LSW-KCl only.

Core2:

The ionic composition of the effluents taken out during flooding of Core2 is shown in *Figure 31* (Ca, Mg, K and Na) and Figure 32 (Ba and Sr). Both FW2 injection and LSW-KCl injection are shown in the figures on the left, and only LSW-KCl flooding is shown in the figures on the right. The concentrations are plotted with respect to PV injected. Ca was adsorbed by the rock in the beginning of the FW2 injection, but stabilized at injected level rather quickly. This indicates that the FW2 was not in equilibrium with the formation. When changing to LSW-KCl, the Ca concentration remained above the injected level throughout the entire flooding. Also a small peak in Ca concentration was observed after about 17 PV had been injected. The variations in ion concentrations (Ca and Mg concentration increasing when Ba and Sr concentration decreased and vice versa) indicate that Ca was being released due to ion exchange.

At the beginning for the FW2 injection, Mg was retained by the rock, as shown in *Figure 31*. After about 2 PVs had been injected, the Mg concentration had stabilized at injected level. When LSW-KCl was injected, the Mg concentration remained at a higher level than injected all through the flooding. This indicates that also Mg was being released.

The K concentration stabilized at injected level almost immediately when FW2 was injected. When switching to LSW-KCl, some K was released before the concentration was reduced to a value lower than injected. This indicated that K was being retained by the rock, replacing Ca, Mg, Sr, and Ba.

As shown in *Figure 31*, Na was being retained by the rock initially, when FW2 was injected. The concentration then stabilized at injected level. When LSW-KCl was injected, the Na concentration remained above injected level.

The concentration of Sr showed a small dip at the beginning of the FW2 injection, as seen in *Figure 32*, indicating that some Sr was retained by the core. When changing to LSW-KCl, the Sr concentration stayed above injected concentration until the end of the injection. This indicates that Sr was being released by the formation.

During the FW2 injection, the Ba concentration was initially much lower than injected value, indicating that Ba was being retained. See *Figure 32*. The concentration stabilizes at injected level after about 5 PV. When changing to LSW-KCl, a small amount of Ba was being released initially, before the concentration stabilized at approximately injected level.

During LSW-KCl injection, STO was slowly produced all the way through the injection period. This might have been caused by divalent ions being replaced by K all through the LSW-KCl injection. The amount of Ca and Mg that was released in Core 2 was smaller than in Core1.

Figure 31 - Effluent concentrations of Ca, Mg, K and Na from Core2. Figures on the left show both FW2 and LSW-KCl injection, while figures on the right show LSW-KCl injection only.

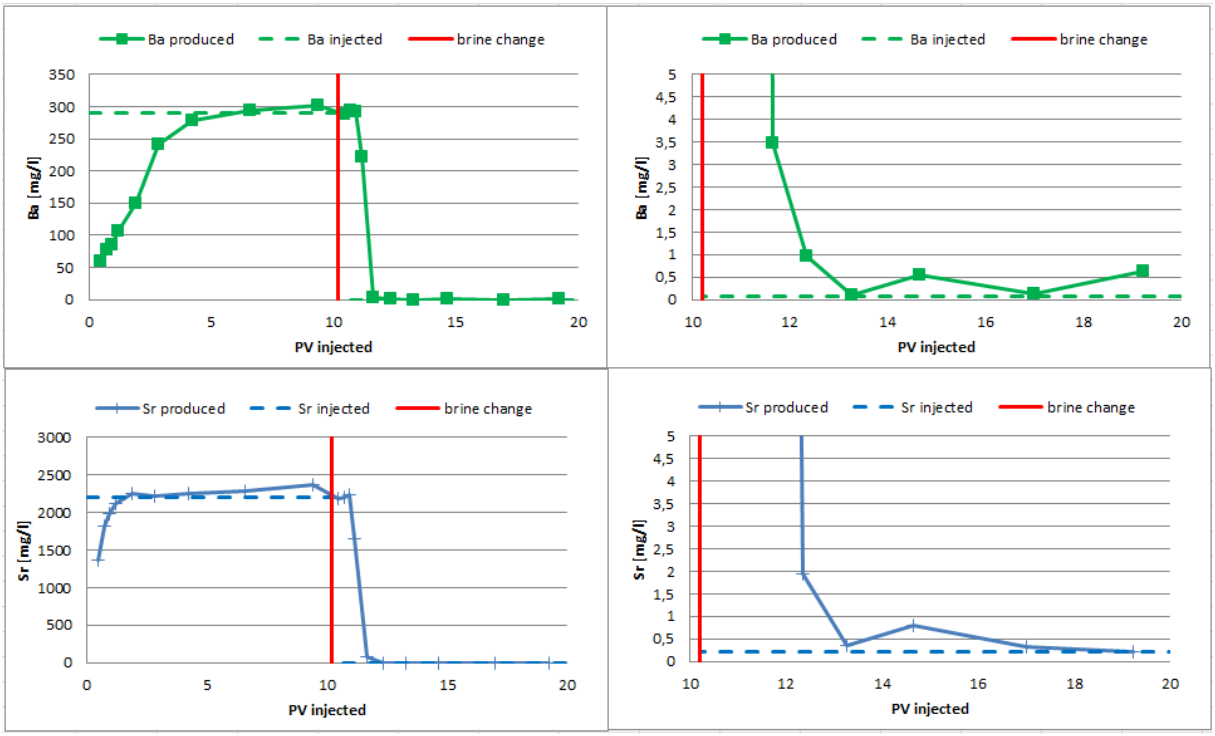

Figure 32 - *Effluent concentrations of Ba and Sr from Core2. Figures on the left show both FW2 and LSW-KCl injection, while figures on the right show LSW-KCl injection only*

Core3:

The ionic compositions of the effluents from Core3 are shown in *Figure 33* (Ca, Mg, K and Na) and *Figure 33* (Ba and Sr). Figures on the left side show both FW3 and LSW-KCl injection, and figures on the right give a closer look of the LSW-KCl injection. In the beginning of the FW3 injection, early variations in effluent concentrations indicate that FW3 was not in equilibrium with the rock. The Ca concentration showed a peak before it stabilized at injected concentration. This indicates release of Ca that might be caused by dissolution of calcite. As shown by *Figure 29* and *Figure 30*, this increase in Ca concentration was also seen in the experiments performed by Fjelde et al. (2012). When LSW-KCl was injected in Core3, Ca was being released, because the produced concentration was higher than injected level until the end of the flooding (see *Figure 33*).

During FW3 injection Mg was initially being retained. See *Figure 33*. The effluent concentration was lower than injected first, before stabilizing at injected level. When LSW-KCl was injected Mg was released by the rock, and injected level was not reached until the end of the flooding.

As shown by *Figure 33*, Na was retained by the rock initially when FW3 was injected. The concentration than stabilized at injected level. When LSW-KCl was injected, the Na concentration remained above injected level, indicating that Na was released.

During FW3 injection the K concentration shows a peak initially, before it stabilized at injected level. See *Figure 33*. The peak was not seen in Core2, indicating that some K might have been replaced by Ba. When LSW-KCl was injected, some K was released before the concentration was reduced to a value lower than injected, indicating that K was retained replacing Ca, Mg, Ba and Sr.

As shown by *Figure 34*, the Sr concentration was kept at injected level all through the FW3 injection. The retention of Sr in Core2 was not seen in Core3, indicating that the elevated Ba concentration caused less Sr to be retained by the core. When LSW-KCl was injected, the Sr concentration was higher than injected all through the flooding, indicating that Sr was being released.

Ba was retained initially when FW3 was injected. See *Figure 34*. The effluent level reached injected level faster than in Core2, which would be expected as the injected concentration was higher. When LSW-KCl was injected, some Ba was released, before effluent level reached injected level.

During LSW-KCl injection, the amount of divalent ions being replaced by K in Core3 was higher than in Core2. This caused some additional oil to be produced. However, the amount of additional oil that was produced from Core3 was smaller than from Core2. This might be because the S_o reached in Core3 after injection of FW3 was much lower than the S_o reached by the two other cores after FW injection, and the potential for LSWF was reduced.

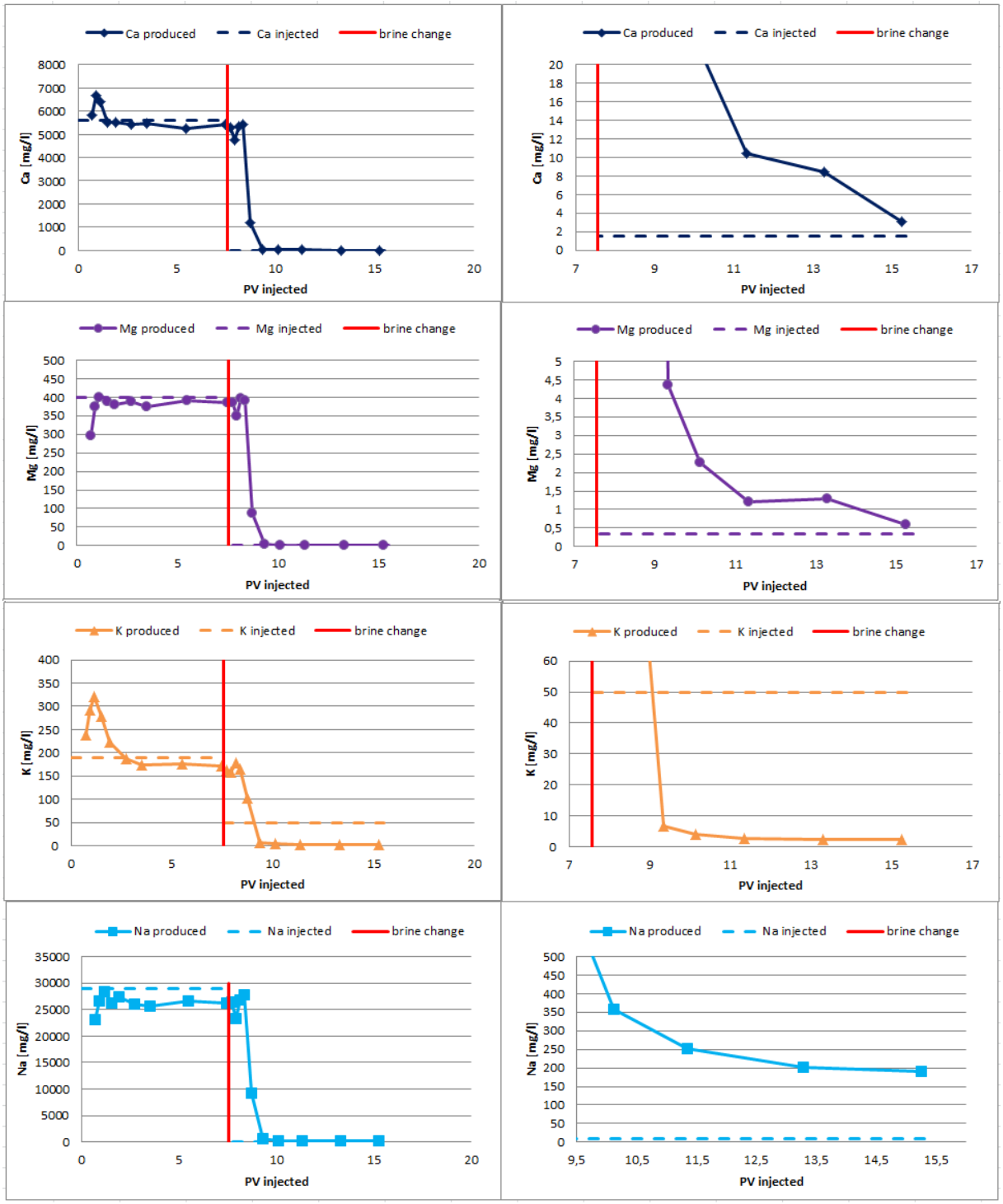

Figure 33 - Effluent concentrations of Ca, Mg, K and Na from Core3. Figures on the left show both FW2 and LSW-KCl injection, while figures on the right show LSW-KCl injection only

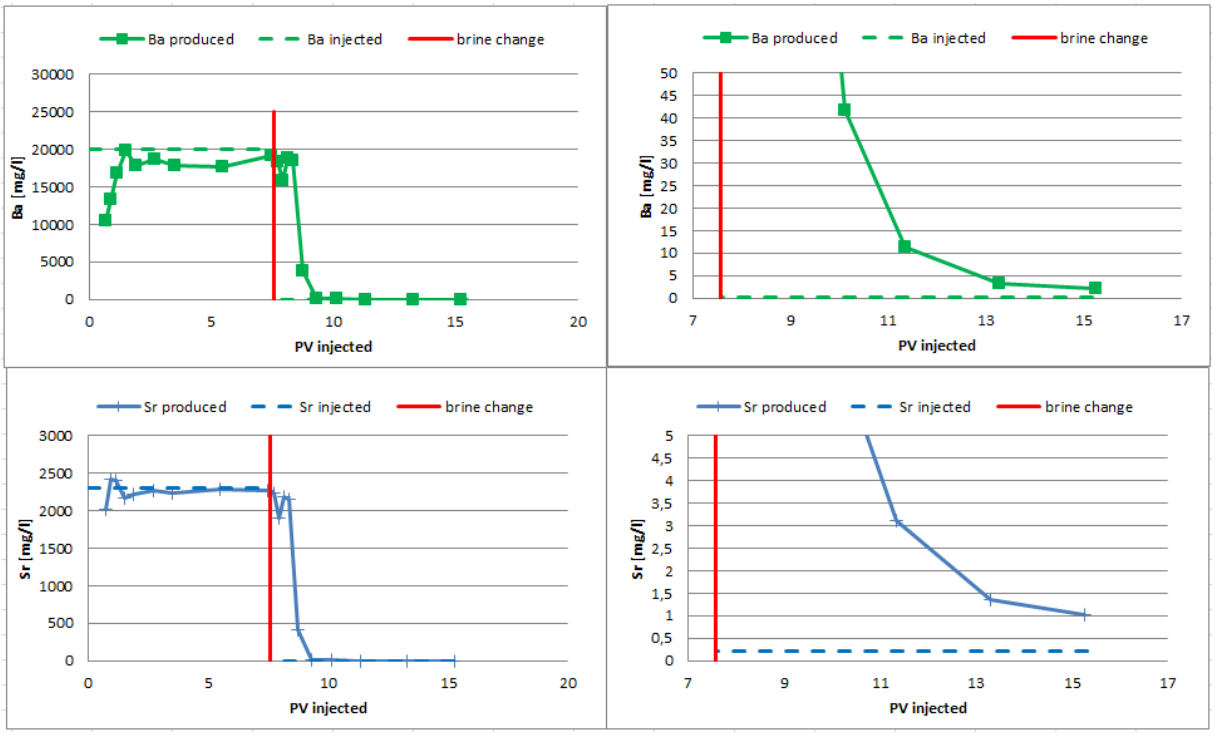

Figure 34 - Effluent concentrations of Ba and Sr from Core3. Figures on the left show both FW3 and LSW-KCl injection,while figures on the right show LSW-KCl injection only

6 Discussion

During the saturation of the cores, both the simulation and the experimental results show that varying the concentrations of Ba and Sr will have an effect on the reactions between the brine and the rock. In the literature it has been claimed that both Ba and Sr will have higher affinity to clay than Ca, Mg and K at equal concentrations (IDS 1982, Suarez and Zahow 1989, Bennet 2013). Suijkerbuijk et al. (2012) showed that the type of ions that are adsorbed on a clay surface will have an effect on the wettability of the rock. It was therefore expected that increasing concentration of Ba and Sr in the FW would cause more of these ions to be adsorbed, and hence alter the wettability. In this study, the simulation results showed that the amount of divalent cations retained on the clay surface would increase with increasing Ba and Sr concentration in the FW, and the experimental results indicated that higher concentrations of Ba and Sr will lead to a more water wet system initially.

In the literature, mixed wet systems have been shown to yield lower S_{or} values than water wet systems (Jadhunandan and Morrow 1995). The production is however slower, water breaks through earlier and higher volume of injected water is needed to reach S_{or}. One would therefore expect faster production and higher S_{or} when wettability is altered toward more water-wet. This was the case when comparing Core1 and Core2, but Core3 reached a much lower S_{or} after FW flooding than both of the other cores (See *Table 10*). However the water relative permeability at the end of the FW floodings of Core2 and Core3 were of similar value. And as S_{or} was lower in Core3 than Core2, this indicated that Core3 was more water wet. This seemed to be caused by more Ca and K ions being replaced by Ba ions in the beginning of the FW3 injection than in the injection of FW2.

On a field scale, the most important average S_o value is the one reached when the production is no longer economically feasible. For a mixed wet system the amount of water that has to be injected to reach the true S_{or} is higher than for a more water wet system (Jadhunandan and Morrow 1995). Therefore production might be ended before the true S_{or} is reached. Altering the wettability towards more water wet will probably increase S_{or}, however, k_{ro} will increase and the oil will be produced faster. This might mean that the average remaining oil saturation at end of production will be lower for a water wet system than for a mixed wet system. In the experiments performed here, it was shown that increasing the Ba and Sr concentrations will lead to a more water wet system. The extreme concentration of Ba would be the most beneficial for fast oil recovery. However, this result may not be of big relevance as the Ba

concentration used was much higher than what will be found in a reservoir. The change towards more water wet was however also noticeable in the core saturated with a normal Ba concentration and a high Sr concentration. This indicated that leaving out Ba and Sr from the FW used in experimental studies might lead to an unrepresentative initial wettability.

The FW composition was also shown to affect LS potential. According to Fjelde et al. (2013a), LSE will be seen where the amount of divalent ions adsorbed on the clay surface is reduced, and that this should be possible to predict using a simulator. However, the simulation results obtained here indicated that the amount of divalent ions adsorbed by the rock would increase when LSW-KCl was injected, and hence no additional oil production due to the LSW should be expected. The experimental floodings showed that this was not the case, as an increase in oil recovery during injection of LSW-KCl was seen in all three cores. The effect was however larger for Core1 and Core2 indicating that the extreme concentration of Ba in FW3 had a negative effect on the LS potential. At the same time, Core2 showed the best response to the LSWF, indicating that a reasonable concentration of Ba and a high concentration of Sr could have a positive effect.

The difference between Cores 1 and 2 and Core3 was indicated by the simulation results. The amount of K adsorbed in simulation 3 (the Core3 experiment) does not increase in the first cells as expected, the amount of Na released was smaller and in the first cells Ca was being adsorbed instead of Mg and some Ba and Sr were released. Simulation 3 also showed the highest amount of divalent ions adsorbed on the formation. These differences are not seen in the experimental results. The effluent ionic compositions from LSW-KCl flooding of Core3 show that K *was* being retained by the formation. And it would seem also like Core 3 was the one with the highest release of all the divalent ions divalent ions. This might not actually be the case however, as the concentrations of the different ions when LSW injection was started were so much higher than at the end of the injection. Compositional changes equal to the ones seen at the end would be too small to detect in the beginning.

6.1– Further work

For further work, duplicate experiments are recommended to confirm the results and conclusions made in this study. Systematic in Ba and Sr concentrations should also be tested as the effect of increased Sr or Ba concentration alone has not been investigated. It might also be useful to test Ba concentrations somewhere between the concentrations used here, as the

high value used (300 ppm) was lower than the highest values reported in the literature (2180 ppm), and the extreme value is not likely to be seen in any reservoir (Merhah and Yassin 2007).

In this work, only one type of sandstone, one basic FW and one crude oil has been used. The reaction between the ions in brine and the formation can vary with different mineral compositions, and also by the distribution of the minerals present. It would therefore be useful to test the effects on different COBR systems.

7 Conclusions

Based on simulations and experimental studies of cores saturated with FW containing three different Ba and Sr concentrations, the following conclusions have been made:

Leaving out Ba and Sr from synthetic FW used in the lab will have an effect on the obtained initial wettability of the rock. This could cause an unrepresentative image of what is actually going on in the formation. In the work done here, both production profiles and end point relative permeability calculations indicate that increasing concentration of Ba and Sr in the FW will lead to a more water wet system initially.

Ion composition of the FW will have an effect on the potential for LSWF. The largest LSE effect is seen in the core containing high, but reasonable concentrations of Ba and Sr, both indicated by additional production in LSWF as well as increased $k_{rw}(S_{or})$.

The presence of Ba only has a positive effect on the LS potential up to a certain level. The core saturated with FW containing an extreme concentration of Ba (19000 ppm) showed a much lower response to the LSW.

The simulations gave a correct image regarding Core3 being different, but regarding a pre evaluation of the LS potential, looking at the amount of divalent ions on the surface, it did not indicate that LSWF would yield any extra production.

8 References

Abdallah, W., Buckley, J.S., Carnegie, A., Herold, J.E.B., Fordham, E., Graue, A., Habashy, T., Seleznev, N., Signer, C., Haussain, H., Montaron, B. and Ziauddin, M. 2007. *Fundamentals of Wettability*. Published in Oilfield Review, Volume 19, Version 2.

Agbalaka, C., Dandekar, A.Y., Partil, S.L., Khantaniar, S. and Hemsath, J.R. 2008. The Effect of Wettability on Oil Recvery: A Review. SPE 114496. Presented at the SPE Oil and Gas Conference and Exhibition, Perth, Australia, 20-22 October 2008.

Anderson, W.G. 1986. Wettability Literature Survey – Part 1: Rock/Oil/Brine Interactions and the Effects of Core Handling on Wettability. SPE 13932. *Journal of Petroleum Technology*, Volume 38, Number 10 1125-1144.

Austad, T., RezaeiDoust, A. and Puntervold, T. 2010. Chemical Mechanism of Low Salinity Waterflooding in Sandstone Reservoirs. SPE 129767. Presented at the SPe Improved Oil Recovery Symposium, Tulsa, Oklahoma. 24-28 April.

Bavière, M. 1991. *Basic Consepts in Enhanced Oil Recovery Processes*. Oxford, Published for the Society of Chemical Industry by Blackwell.

Bennet P. downloades 2013 Surface Chemistry and ion exchange. Lecture notes from the Chemical Hydrology course at the University of Texas.

Bernard, G.G. 1967. Effect of Floodwater Salinity on Recovery of Oil on Cores Contatining Clays. Presentes at the 38th annual California Regional Meeting of the Society of Petroleum Engineers of AIME. Los Angeles, California 26-27 October.

Castellan, G.W., 1983. *Physical chemistry*, 3rd edition, Addison-Wesley Publishing Company, Reading, Massachusettes

da Costa Ferriera, J. 2012. Low Salinity Effect After Sea Water Flooding in Sandstone Reservoir. Master thesis, University of Stavanger.

Dolcater, D.L., Lotse, E.G., Syers, D.K. and Jackson, M.L. 1968. Cation Exchange Selectivity for Some Clay Sized Minerals and Soil Materials. *Soil Sci. Soc. Am. Proc*. 32 795-798.

Donaldson, E. and Alam, W. 2008. *Wettability* volume 978. Gulf Publishing Company.

Engler, T. W. 2012 Formation evaluation lecture notes from the New Mexico Institute of Mining and Technology http://infohost.nmt.edu/~petro/faculty/Engler571/Chapter7-Capillarypressure.pdf

Fjelde, I., Aasen, S.M. and Omekeh, A. 2012. Low Salinity Water Flooding Experiments and Interpretation by Simulations. SPE 154142. Presented at the Improved Oil Recovery Symposium in Tulsa, Oklahoma 14-18 April.

Fjelde, I., Aasen, S.M., Omekeh, A. and Polanska, A. 2013a. Secondary and Tertiary Low Salinity Water Floods: Experiments and Modelling. SPE 164920-MS. Presented at the Conference and Exhibition incorporating SPE Europec held in London, United Kingdom 10-13 June.

Fjelde, I. 2013b. Personal communication.

Glover, P. 1997. Formation Evaluation Lecture Notes. From the Formation Evaluation Course at the University of Aberdeen.

Green, D.W. and Willhite, G.P. 1998 *Enhanced Oil Recovery*. SPE Textbooks series 6. Henry L. Doherty Memorial Fund of AIME. Society of Petroleum Engineers, Richardson, Texas USA.

IDF, 1982. *Clay Chemistry*, Technical Manual for Drilling, Completion and Workover Fluids. International Fluids Limited.

Jadhunandan, P. 1990. Effects of Brine Composition, Crude Oil and Aging Conditions on Wettability and Oil Recovery. PhD dissertation. New Mexico Institute of Mining and Technology.

Jadhunandan, P.P. and Morrow, N.R. 1995. Effect of Wettability on Waterflood Recovery for Crude-Oil/Brine/Rock systems. *SPE Reservoir Engineering, February* (40-46).

Lager, A., Webb, K.J., Black, C.J.J, Singleton, M., Sorbie, K.S. 2006. Low Salinity Oil Recovery – An Experimental Investigation. SCA2006-36. Presented at the International Symposium of the Society of Core Analysts held in Trondheim, Norway.

Lager, A., Webb, K.J., Collins, I.R., Richmond, D.M. 2008. $LoSal^{TM}$ Enhanced Oil Recovery: Evidence of Enhanced oil Recovery at the Reservoir Scale. SPE 113976. Presented at the SPE/DOE Improved Oil Recovery Symposium held in Tulsa, Oklahoma, USA.

Lee, S.Y., Webb, K.J. et al.. 2010 Low Salinity Oil Recovery – Increasing Understanding of the Underlying Mechanisms. SPE 129722. Presented at the SPE Improved Oil Recovery Symposium held in Tulsa, Oklahoma, 24-28 April.

Lighthelm, D.J., Gronsveld, J., Hofman, J.P., Brussee, N.J., Marcelis, F. and van der Linde, H.A. 2009. Novel Waterflooding Strategy by Manipulation of Injected Brine Composition. SPE 119835. Presented at EUROPEC/DOE Conference and Exhibition held in Amsterdam, The Netherlands 8-11 June.

McGuire, P.L., Chatham, F.K., Paskvan, F.K., Sommer, D.M. and Carini, F.H. 2005. Low Salinity Oil Recovery: An Exciting New EOR Opportunity for Alaska's North Slope. SPE 93903. Presented at the SPE Western Regional Meeting held in Irvine, California, USA.

Merdhah, A.B. and Yassin, A.A.M. 2007. Barium Sulfate Scale Formation in Oil Reservoir During Water Injection at High-Barium Formation Water. Published in Journal of Applied Sciences 7 (17) 2393-2403.

Morrow, N.R., Valat, M. and Yildiz, H. 1996. Effect of Brine Composition on Recovery of an Alaskan Crude Oil by Waterflooding. Paper 96-94. Presented at the Technical Meeting of the Petroleum Society in Calgary, Alberta, Canada.

Morrow, N.R., Tang, G., Valat, M. and Xie, X. 1998. Prospects of Improved Oil Recovery Related to Wettability and Brine Composition. Journal of Petroleum Science and Engineering 20. (267-276).

Morrow, N. and Buckley, J. 2011. Improved Oil Recovery by Low Salinity Waterflooding. SPE 129421. *Distinguished Author Series*, Volume 63, Number 5, 106-112.

Nasralla, R.A., and Nasr-El-Din, H.A. 2011. Impact of Electrical Surface Charges and Cation Exchange on Oil Recovery by Low Salinity Water. SPE 147937. Presented at the SPE Asia Pacific Oil and Gas Conference and Exhibition held in Jakarta, Indonesia.

Norwegian Petroleum Directorate (2012) from http://www.npd.no/en/About-us/Information-services/Dictionary/.

Parkhurst, D., Appelo, C.A.J. 1999. *Users Guide to PHREEQC (version 2) – a Computer Program for Speciation, Batch-reaction, One-dimensional Transport and Inverse Geochemical Calculations.* U.S Department of the Interior.

Omekeh, A., Friis, H.A., Fjelde, I. and Evje, S. 2012. Modeling of Ion-Exchange and Solubility in Low Salinity Waterflooding. SPE 154144. Presented at the 18th SPe Improved Oil Recovery Symposium held in Tulsa, Oklahoma, USA, 14-18 April.

Omekeh, A.V. 2013. A Study of Low Salinity Effects: Experiments and Moldeling. PhD dissertation. University of Stavanger.

RezaeiDoust, A. 2011. Low Salinity Waterflooding in Sandstone Reservoirs: a Chemical Wettability Alteration Mechanism. PhD dissertation. University of Stavanger.

Seccombe, J.C., Lager, A., Webb, K., Jerauld, G. and Fueg, E. 2008. Improving Waterflood Recovery: $LoSal^{TM}$ EOR Field Evaluation. SPE 113480. Presented at the SPE/DOE Improved Oil Recovery Symposium held in Tulsa, Oklahoma 20-23 April.

Suijkerbuijk, B.M.J.M., Hofman, D.J., Ligthelm, D.J., Romanuka, J., Brussee, N., van der Linde, H. A. and Marcelis, A.H.M. 2012. Fundemental Investigations Into Wettability and Low Salinity Flooding by Parameter Isolation. SPE 154204. Presented at the SPE Improved Oil Recovery Symposium held in Tulsa, Oklahoma, USA, 14-18 April 2012.

Suarez, D.L. and Zahow, M.F. 1989.Calcium-Magnesium Exchange Selectivity of Wyoming Montmorillonite in Chloride, Sulfate and Perchlorate Solutions. Published in Soil. Sci. Soc. Am. J. 53:52-57.

Tang, G.Q. and Morrow, N.R. 1997. Salinity, Temperature, Oil Composition and Oil Recovery by Waterflooding. SPE 36680. Presented at the Technical Conference and Exhibition held in Denver, Colorado, USA.

Tang, G.Q. and Morrow, N.R. 1999. Oil Recovery by Waterflooding and Imbibition – Invading Brine Cation Valency and Salinity. SCA9911. Presented at the International Symposium of the Society of Core Analysts held in Golden, Colorado, USA.

Tree Fruit Soil and Nutrition (2004): http://soils.tfrec.wsu.edu/webnutritiongood/soilprops/04CEC.htm

www.groundwaterresearch.com.au

Zolotukhin, A.B. and Ursin, J-R. 2000. *Introduction to Petroleum Reservoir Engineering.* Kristiansand Høyskoleforlag.